Liquid Crystals
Publication details, including instructions for authors and subscription information:
http://www.informaworld.com/smpp/title~content=t713926090

Magnetic field induced bistability in distorted nematic ground states

U. D. Kini[a]
[a] Raman Research Institute, Bangalore, India

To cite this Article Kini, U. D.(1994) 'Magnetic field induced bistability in distorted nematic ground states', Liquid Crystals, 17: 1, 65 — 93
To link to this Article: DOI: 10.1080/02678299408036550
URL: http://dx.doi.org/10.1080/02678299408036550

LIQUID CRYSTALS, 1994, VOL. 17, NO. 1, 65–93

Magnetic field induced bistability in distorted nematic ground states

by U. D. KINI
Raman Research Institute, Bangalore-560 080, India

(*Received 14 June 1993; accepted 22 November 1993*)

Previous theoretical studies are extended to consider bistability of director orientations induced by changing the tilt of a magnetic field applied to a nematic sample. The ground state configuration which is assumed to be twisted, with the director tilted at the sample planes, can be one of two kinds—S_1 and S_2. The rigid anchoring hypothesis is employed throughout. When the field is sufficiently strong there occur two independent branches over which the distortion varies as the magnetic tilt is changed and these branches generally overlap over the bistable region. When the ground state twist is high enough, the bistable region can disappear altogether leaving a gap of no overlap between the two branches. Linear stability analysis shows that the static orientation tends to become unstable against linear perturbations when the magnetic tilt crosses the edges of the gap. It is possible that the distortion changes irreversibly from the S_1 type (or S_2 type) to one of S_2 type (or S_1 type) causing a considerable lowering of the overall twist. Results for positive diamagnetic anisotropy materials ($\chi_A > 0$) are compared with those for negative χ_A materials. When the ground state is of the S_2 type, a sufficiently strong field applied along certain directions can produce a transition at a threshold above which the distortion becomes asymmetric relative to the sample centre. The case of chiral nematics and that of weak anchoring are briefly reviewed.

1. Introduction

Nematic and cholesteric liquid crystals have been the subject of basic research because of their many fascinating anisotropic physical properties [1–5]. For the purposes of describing macroscopic phenomena, it is convenient to introduce the unit, non-polar, director vector field **n** which describes the preferred direction of orientation at a given point. The direction of alignment of **n** at surfaces can be controlled by suitable surface treatment. In a given sample, the orientation of **n** can be affected by the application of external electric and magnetic (**H**) fields. By exploiting the optical anisotropy of these materials and by proper use of polarized light, it has been possible to develop display devices based on various electro-optic effects ([6]; for recent reviews on the subject of displays and applications see for instance [7] and references therein). It is the strong interaction between the material and the applied electric field which is responsible for making these devices work at reasonably low voltages.

The effects of external fields on the director orientation in nematic and cholesteric samples are well understood on the basis of continuum theory [1–5]. This theory has also been extensively used [7] for understanding the working of electro-optic devices and also for improving the performance of such devices via mathematical simulation.

Limitations of the earlier twisted nematic devices have been removed by the use of supertwisted nematic configurations [8–10]. In these devices the director field in the ground state is twisted through more than $\pi/2$ radians by the addition of chiral dopants. The helical axis is aligned normal to the plates between which a voltage can be

0267-8292/94 $10·00

applied and by suitable surface treatment, the director at the sample planes is also pretilted away from the homogeneous alignment (a recent review on these devices can be found in [10]). Electrical switching between bistable orientation patterns [11] has also been suggested [12] as a possible means of building display devices.

In all the above cases, an electric field is employed and the direction of the field is normal to the plates. It should be interesting to study the effect of changing the direction of the applied electric field on the director orientation in such devices, but this is not straightforward in practice as it would involve applying voltages simultaneously along, as well as normal to, the sample planes. It is well known, for instance, that an electric field applied along the sample planes can lead to a discontinuous Fréedericksz transition, bistability, static periodic deformations [13], etc. These effects are mainly brought about by the high electric susceptibilities of the material which cause considerable modification of the electric field in the presence of director gradients inside the sample.

A magnetic field, in the other hand, is less interesting from the viewpoint of device applications, but is more convenient for study of director distortions, as its direction of application can be chosen freely. The action of a magnetic field can also lead to interesting effects. For instance, the change in tilt of a sufficiently strong field can lead to bistable behaviour [14, 15] in which the variation of average orientation as a function of the magnetic tilt falls on two separate branches which overlap. In the bistable region, therefore, there can exist two separate distortion states with different deformation free energy, each state being the result of the particular 'history' of variation of the magnetic tilt. Attempts have been made [15] to utilize these effects to estimate elastic constants. It appears [16] that the language of catastrophe theory can also be used to understand the discontinuous transitions which occur at the edges of the bistable region.

The continuum theory has been employed [17, 18] to study the occurrence of bistability for different parameters including the director tilts at the boundaries, director anchoring strengths at the sample planes, orientation of the magnetic plane etc; the studies have also been extended to nematics having negative χ_A, leading to the investigation of transitions between distortions of different kinds. Perturbation analysis has shown that in the presence of bistability, the static solution on one of the branches can become unstable when the magnetic tilt approaches the edges of the bistable region. This lends indirect support to earlier observations [14–16] of discontinuous orientational changes at the peripheries of the bistable region.

In these studies, the effect of a ground state twist on the occurrence of bistability has not been investigated in detail. The ground state of a nematic can be twisted, in most cases, by a rotation of one of the sample planes relative to the other or by the addition of chiral dopants or by a combination of these two processes. It seems interesting to find out how the presence of an overall twist in the ground state will affect the bistability of magnetic field induced distortion under a variation of the magnetic tilt. This should be of special interest, because earlier studies have shown that when the ground state twist caused by intrinsic chirality is sufficiently high, with the helical axis and magnetic field normal to the sample planes, the resulting deformation above threshold may not be homogeneous [19], but periodic [20]. It also seems necessary to include director tilt at the boundaries as one of the relevant parameters.

With this motivation, the mathematical model is briefly described in § 2, while §§ 3 and 4 deal with the results for different ground states of a nematic without intrinsic chirality. In § 5, results for a negative χ_A material are compared with those for a positive χ_A nematic obtained in the earlier sections. Section 6 concludes the discussion.

2. Mathematical model, boundary conditions and method of solution

We follow closely the mathematical model employed in [18]. Let a chiral nematic be confined between plane parallel plates $z = \pm h$ (sample thickness $= 2h$) at which the easy directions of director orientation are given by

$$d_{\pm} = (\cos\theta_{\pm}\cos\phi_{\pm}, \cos\theta_{\pm}\sin\phi_{\pm}, \sin\theta_{\pm}) \tag{1}$$

in rectangular cartesian coordinates. The magnetic field impressed on the sample

$$\mathbf{H} = (HC_{\alpha}C_{\beta}, HC_{\alpha}S_{\beta}, HS_{\alpha}); \qquad C_{\alpha} = \cos\alpha; \qquad S_{\beta} = \sin\beta \tag{2}$$

is described by the polar angle α and the azimuthal angle β. Clearly, when $\alpha = \pi/2$, $\mathbf{H}$ is directed along the z axis (normal to the plates) and the azimuthal angle is of no consequence; when $\alpha = 0$, $\mathbf{H}$ lies in the xy plane. The resulting director distortion is assumed to be homogeneous and mono-domain so that

$$\mathbf{n} = (C_{\theta}C_{\phi}, C_{\theta}S_{\phi}, S_{\theta}); \qquad \theta = \theta(z); \qquad \phi = \phi(z). \tag{3}$$

Essentially this assumes that we concentrate on a region of the sample away from the lateral edges and that formation of domains having homogeneous deformations of different parity separated by domain walls is ignored. The equilibrium configuration is characterized by the total free energy density W_V and the vanishing of the two independent components of the total bulk torque $\boldsymbol{\Gamma}$:

$$W_V = f_1(\theta)\phi_{,z} + [\{f_2(\theta)\theta_{,z}^2 + f_3(\theta)\phi_{,z}^2\}/2] + f_4(\theta, \phi); \tag{4}$$

$$\begin{aligned}
\Gamma_{\theta} &= f_2(\theta)\theta_{,zz} + [(df_2/d\theta)\theta_{,z}^2 - (df_3/d\theta)\phi_{,z}^2]/2 \\
&\quad - (\partial f_4/\partial\theta) - (df_1/d\theta)\phi_{,z} = 0; \\
\Gamma_{\phi} &= f_3(\theta)\phi_{,zz} + (df_1/d\theta)\theta_{,z} + (df_3/d\theta)\theta_{,z}\phi_{,z} - (\partial f_4/\partial\phi) = 0;
\end{aligned} \tag{5}$$

$$\left.\begin{aligned}
f_1(\theta) &= -k_2C_{\theta}^2; \qquad f_2(\theta) = K_1C_{\theta}^2 + K_3S_{\theta}^2; \qquad f_3(\theta) = C_{\theta}^2(K_2C_{\theta}^2 + K_3S_{\theta}^2); \\
f_4(\theta, \phi) &= -\mu_0\chi_A H^2[C_{\alpha}C_{\theta}\cos(\beta - \phi) + S_{\alpha}S_{\theta}]^2/2
\end{aligned}\right\} \tag{6}$$

where K_1, K_2, K_3, are the splay, twist and bend curvature elastic constants, respectively; $k_2 = 2\pi K_2/P_0$; P_0 is the equilibrium pitch of the unconstrained chiral nematic ($k_2 = 0$ for a non-chiral nematic); $\theta_{,z} = d\theta/dz$ etc. The equilibrium configuration (3) can be obtained by solving (5) with suitable boundary conditions. Then by integrating W_V (4), the total free energy can be estimated. The inclusion of the surface free energy density [21] leads to a more realistic set of boundary conditions (see equations (2.5) and (2.7) in [18]). The inclusion of finite anchoring energy brings into the picture the anchoring strengths at the boundaries as additional parameters. For the sake of simplicity, therefore, we adopt the rigid anchoring hypothesis (equation (2.8) in [18]) so that

$$\theta(z = \pm h) = \theta_{\pm}; \qquad \phi(z = \pm h) = \phi_{\pm}. \tag{7}$$

The solution of (5) and (7) is conveniently effected by using the orthogonal collocation method [22] with the zeros of the 24th order Legendre polynomial as collocation points [23]. Then the integration of W_V to calculate the total free energy of the sample can be achieved by employing the Gaussian quadrature technique [23] in tandem. In the next few sections we shall study the results obtained for different cases.

3. Results for the case $k_2 = 0$; no intrinsic chirality

It is assumed that the material is a nematic without a chiral dopant. Before making detailed calculations, it is necessary to fix the *ground state* configuration (i.e. the director orientation in the absence of external fields). A reference field should also be defined so that a suitable, dimensionless reduced field can be used to indicate the magnitude of the field strength. To start with, it is assumed that

$$\phi_{\pm} = \pm\phi_0; \qquad \theta_{\pm} = \theta_0. \tag{8}$$

This shall be called the *ground state* S_1 (in § 4 another ground state is encountered). According to (8), the twist angle $\phi(z)$ is antisymmetric and the splay–bend angle $\theta(z)$ is symmetric relative to the sample centre when $H = 0$; at $z = 0$, $\theta(z)$ takes the extremum value, say, θ_M, but $\phi(z) = 0$. This also means that the director at the sample centre is aligned along the x axis. *For reasons of convenience, symmetry, antisymmetry or non-symmetry will always be referred relative to the sample centre* ($z = 0$).

In the special case $\theta_0 = 0$, the S_1 ground state reduces to the simple twisted nematic with $\theta(z) = 0$ and $\phi(z) = \phi_0 z$. The non-polarity of $\mathbf{n}$ imposes the restriction that $|\phi_0| < \pi/4$ in order that the ground state may have a single domain twist distortion. If the material has $\chi_A > 0$ (this is assumed to be true throughout the present work, except, as in § 5, where it is explicitly stated to be otherwise), a field along z (i.e., $\alpha = \pi/2$) leaves the ground state unchanged provided that $H < H_F$ with [19]

$$H_F = [\{K_1(\pi^2/4h^2) + (K_3 - 2K_2)(\phi_0^2/h^2)\}/\mu_0\chi_A]^{1/2}. \tag{9}$$

This seems to be a convenient field with respect to which H can be measured. A reduced field

$$R = H/H_F \tag{10}$$

can now be defined. It should be remembered that H_F is a function of ϕ_0 which is half the total twist in the S_1 ground state. As long as we compare different results obtained for a given ϕ_0, the definition (10) suffices. If, however, we are comparing results for different ϕ_0 in the same diagram (as in § 4.3.), it becomes more appropriate to use a definition of the reduced field in terms of a standard field which is independent of ϕ_0. It has already been shown [17, 18] that under the rigid anchoring hypothesis, the governing equations (5) can be cast into scaled form using (10) and the dimensionless variable $\xi = z/h$. Because of this, some convenient values can be chosen for the sample thickness and χ_A; say, $h = 100\,\mu$m; $\chi_A = 4\pi \times 10^{-7}$ SI units. All angles are measured in radian. The curvature elastic constants for the nematic (E7) are [24],

$$\left.\begin{aligned} &(K_1, K_2, K_3) = (1{\cdot}85,\ 1{\cdot}3,\ 2{\cdot}02) \times 10^{-12}\ \text{N}; \\ &K_1/K_2 = 1{\cdot}423, \qquad K_3/K_2 = 1{\cdot}554; \qquad K_3/K_1 = 1{\cdot}092. \end{aligned}\right\} \tag{11}$$

As will become clear later, it is necessary to compare results for E7 with those obtained for another material, say, 5CB [25],

$$\left.\begin{aligned} &(K_1, K_2, K_3) = (6{\cdot}41,\ 3{\cdot}97,\ 9{\cdot}23) \times 10^{-12}\ \text{N}; \\ &K_1/K_2 = 1{\cdot}615; \qquad K_3/K_2 = 2{\cdot}325; \qquad K_3/K_1 = 1{\cdot}44. \end{aligned}\right\} \tag{12}$$

A significant difference between the data sets (11) and (12) is that the quantity $K_3 - 2K_2$ is negative for the former but positive for the latter. This means that for E7, H_F should be less than the splay Fréedericksz threshold; for 5CB, the splay threshold should be

less than H_F. It seems worth putting this to an experimental test. It must be remembered that the significance of the ratio K_3/K_2, as also its effect on determining the ground state distortion, has already been pointed out [26].

3.1. *Investigation of the stable ground state;* $H=0$

Noting the characteristics of the S_1 ground state, it is clear that this distortion can be obtained by starting with a uniformly tilted orientation in the xz plane

$$\mathbf{n}_0=(\cos\theta_0, 0, \sin\theta_0) \tag{13}$$

involving zero twist ($\phi_0=0$). For definiteness, $\theta_0>0$; it is clear that results for $\theta_0<0$ can be obtained by simple transformations. Remembering that the director is rigidly anchored at the sample planes; it is now assumed that the sample boundaries $z=\pm h$ are rotated about the z axis through $\pm\phi_0$ such that for a given ϕ_0, the total twist in the sample is $2\phi_0$ (again, ϕ_0 is assumed to be positive). As the twist in the sample is increased from zero, the splay–bend distortion also sets in and θ_M changes from θ_0. While the $\theta(z)$ profile is symmetric, the $\phi(z)$ profile is antisymmetric with $\phi(z)$ increasing monotonously from $-\phi_0$ at $z=-h$ to ϕ_0 at $z=h$. Because of this, θ_M is the only quantity of interest here.

Figure 1 (*a*) contains plots of θ_M as a function of ϕ_0 for the E7 material parameters (11). It is found that at a given θ_0, θ_M increases with ϕ_0; when ϕ_0 exceeds a critical value ϕ_C (which is, in general, a function of the material constants and θ_0), θ_M increases sharply and for $\phi_0>\phi_C$, a solution cannot be found for (5) satisfying (7). The non-existence of the solution is deduced when the algorithm used for calculating the θ and ϕ profiles diverges at $\phi_0>\phi_C$. When θ_0 is enhanced (see figure 1 (*a*) curves 2, 3), ϕ_C diminishes. It is thus clear that for a given pre-tilt angle θ_0, the S_1 ground state exists provided that $\phi_0<\phi_C$. We shall postpone, for the moment, answering the question as to what happens to the deformation when ϕ_0 exceeds ϕ_C (see § 4).

It may be checked that identical curves to those in figure 1 (*a*) will result if the sign of ϕ_0 is reversed and θ_M plotted as a function of $-\phi_0$. The curves will also represent the variation of θ_M for negative θ_0 if we replace θ_M by $-\theta_M$ on the y axis.

Figure 1 (*b*) shows the same functional variations as figure 1 (*a*), but for 5CB parameters (12). It is found that up to about $\theta_0=0{\cdot}35$, θ_M actually decreases when ϕ_0 is enhanced (see figure 1 (*b*), curve 1); stable solutions for the S_1 ground state are found to exist even beyond $\phi_0=\pi$. When θ_0 is increased beyond this value (figure 1 (*b*), curves 2, 3) one recovers the same kind of variation obtained of E7.

Figure 1 (*c*) depicts dependence of θ_M on θ_0 at fixed values of ϕ_0 (i.e. at fixed values of the ground state twist). The relevant range is $0<\theta_0<\pi/2$. The results are presented for E7 parameters, but very similar conclusions can be reached at comparable values of ϕ_0 if one employs the 5CB material parameters. As long as the overall twist is small enough (see figure 1 (*c*), curve 1); a stable ground state exists for all θ_0 in the permitted range. When, however, ϕ_0 becomes sufficiently high (figure 1 (*c*), curves 2, 3), stable solutions of (5) satisfying boundary conditions (7) do not appear to exist if $\theta_0>$ some limit θ_C; clearly, the higher the overall twist, the lower the corresponding θ_C.

It is now necessary to study the effect of **H** on the ground state. Once the field is impressed on the sample, $\theta(z)$ and $\phi(z)$ may or may not continue to conform to the symmetries exhibited by the S_1 ground state, depending upon the magnitude and direction of the field. A solution of the governing equations (5) satisfying the boundary conditions (7) shall be referred to as S_1 *distortion or* S_1 *deformation.*

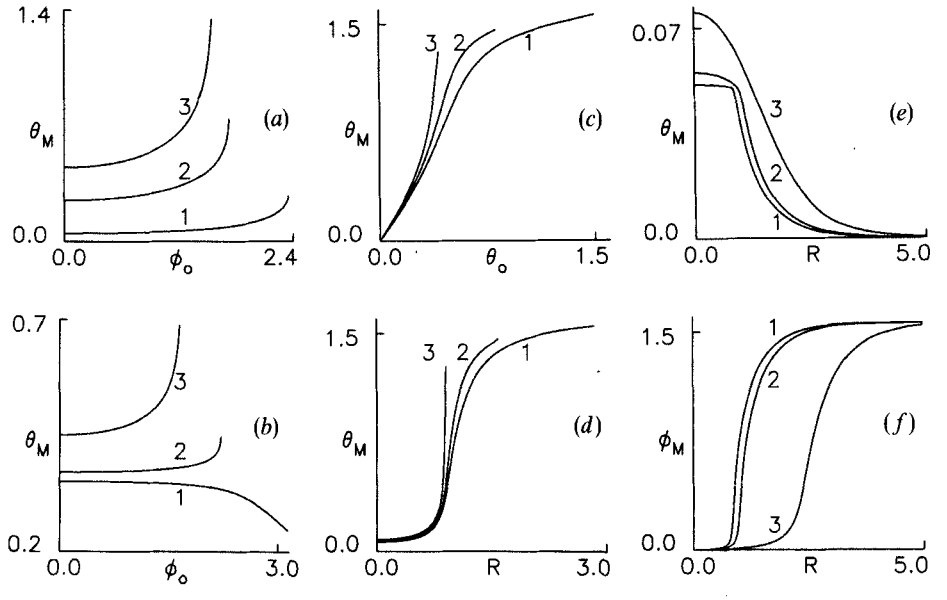

Figure 1. Variation of average deformation with different parameters. The sample planes are $z = \pm h$. In the absence of imposed twist the director is uniformly tilted in the xz plane (13) making an angle θ_0 with the x axis. Except in figure 1 (*b*), material parameters are those of E7 (11). Due to an imposed twist of $2\phi_0$, the S_1 ground state (8) has a combination of splay, twist and bend distortions, with θ taking the extremum value θ_M at the sample centre. In (*a*) and (*c*), the field is zero. (*a*) Plots of θ_M as a function of ϕ_0 for $\theta_0 = (1)$ 0·05 (2) 0·25 (3) 0·45 radian. A stable ground state configuration cannot be found when ϕ_0 exceeds a critical limit ϕ_C. (*b*) θ_M versus ϕ_0 for $\theta_0 = (1)$ 0·35 (2) 0·37 (3) 0·45 radian; the material parameters are those of 5CB (12). The qualitative difference in the behaviour of low and high pre-tilt cases is discernible. (*c*) Variation of θ_M with θ_0 for different ground state twist; $\phi_0 = (1)$ 1·36 (2) 1·46 (3) 1·56 radian. When the ground state twist is sufficiently high, a stable S_1 ground state may not be possible when θ_0 exceeds a critical limit θ_C. Substantially similar curves are obtained for 5CB parameters (see § 3.1.). (*d*) θ_M as a function of the reduced field $R(10)$ when **H** is impressed along z, the sample normal ($\alpha = \pi/2$); $\theta_0 = 0{\cdot}05$ radian. $\phi_0 = (1)$ 1·17 (2) 1·36 (3) 1·56. Similar behaviour is seen for 5CB parameters with $\theta_0 = 0{\cdot}35$ and 0·37 radian. (*e*) and (*f*) Variation of θ_M and ϕ_M with R with **H** acting in the xy plane close to the y axis; $\alpha = 0$ and $\beta = 1{\cdot}56$ radian; $\theta_0 = 0{\cdot}05$. $\phi_M = \phi(z = 0)$. The $\theta(z)$ and $\phi(z)$ profiles are asymmetric. $\phi_0 = (1)$ 0·39 (2) 0·78 (3) 1·5. When the field becomes strong enough, $\theta_M \to 0$ and $\phi_M \to \pi/2$ (see § 3.2.).

3.2. *H along symmetry directions*

It seems advisable to study the effects of applying **H** along the different symmetry directions of the S_1 ground state before considering the effect of changing the magnetic tilt. One of the symmetry directions is, obviously, the z axis ($\alpha = \pi/2$; then, β becomes irrelevant). Clearly, the field applied along z will not affect the symmetry of the director orientation; also, as the director is tilted with respect to the sample planes, a distortion can set in without a threshold.

Plots of θ_M versus the reduced field R are shown in figure 1 (*d*) for a given pretilt of the ground state ($\theta_0 = 0{\cdot}05$) and different twists ϕ_0; the material parameters are those of E7. It is seen that when ϕ_0 is low, θ_M increases monotonically with R and approaches $\pi/2$ when R attains high values. If the overall twist is sufficiently high (see figure 1 (*d*),

curves 2, 3), the increase of θ_M is more rapid, and stable solutions of (5) satisfying (7) do not seem to exist when R exceeds some limit R_{C1}; clearly, the higher the ϕ_0, the lower the corresponding R_{C1}. Calculations for 5CB parameters show that similar curves can be obtained for $\theta_0 = 0{\cdot}35$ and $0{\cdot}37$ radian.

Noting that the director at the sample centre is aligned along the x axis, one can consider two other configurations for applying **H**. As before, we choose values of ground state twist such that ϕ_0 is sufficiently removed from the critical limit ϕ_C. In the first of these, **H** is impressed along the x axis ($\alpha = 0 = \beta$). In this case an increase of R will cause the director field to rotate towards **H** without change in the symmetries of the angles θ and ϕ, so that one can expect a monotonic decrease of θ_M when R is enhanced.

In the other related configuration we consider **H** applied along the y axis ($\alpha = 0$, $\beta = \pi/2$). When R is increased, the director field in the sample gets deformed. It must be remembered that the director at the sample centre is oriented along x (normal to **H**). For this reason, the director distortion changes with increasing R in such a way that the symmetry of $\theta(z)$ and the antisymmetry of $\phi(z)$ are preserved; naturally, θ_M will diminish when R is enhanced.

The situation becomes more interesting when **H** lies in the xy plane, but is not directed exactly along the y axis. Then with increasing R, a non-zero magnetic torque will be experienced by the director at the sample centre. In this case, the director profile will become asymmetric—neither will $\theta(z)$ be symmetric nor will $\phi(z)$ remain antisymmetric. In particular, $\phi_M = \phi(z = 0)$ will not remain zero. In earlier work [18], when asymmetric profiles of θ and ϕ were encountered, θ_M and ϕ_M were used to represent the average deformation in the sample. For the sake of consistency, this is done in the present work too.

Figures 1 (*e*) and (*f*) contain the variations of θ_M and ϕ_M as functions of R with $\alpha = 0$, $\beta = 1{\cdot}56$; E7 parameters are used with $\theta_0 = 0{\cdot}05$ radian. It is seen that when the field is sufficiently strong, $\theta_M \to 0$ and $\phi_M \to \pi/2$. It is worth remarking (figures 1 (*e*) and (*f*), curves 1, 2) that when the ground state twist is not very high, the initial diminution in θ_M and increase in ϕ_M are quite sharp. Calculations for 5CB parameters with $\theta_0 = 0{\cdot}35$ or $0{\cdot}37$ radian yield very similar curves. It should be obvious that for $\beta = 1{\cdot}58$, the sign of ϕ_M will reverse; otherwise the results are qualitatively similar.

When the ground state twist is increased further ($\phi_0 = 1{\cdot}95$ radian; figures 2 (*a*) and (*b*), curve 3), the nature of the variation of distortion with R is found to be quite different from that shown in figures 1 (*e*) and (*f*); while θ_M diminishes with increasing R, ϕ_M is found to vary but little. This indicates that for some intermediate ϕ_0, a change over in behaviour can be expected. This is indeed found to happen (figures 2 (*a*) and (*b*), curves 1, 2) for ϕ_0 close to β. It is found that ϕ_M either increases sharply (curve 1) or diminishes after an initial increase (curve 2). This behaviour can be seen more clearly for 5CB (figures 2 (*c*)–(*f*)). Interestingly, the θ_M variation does not show any drastic difference under a small increase in the overall twist.

It is easy to perceive intuitively why the above behaviour is seen if the directions of the field, and also those of the director alignment at the boundaries, are explicitly expressed in terms of quadrants in the xy plane. Let β be $1{\cdot}56$ radian; then **H** can be said to lie in the first (or third) quadrant. If $\phi_0 = 1{\cdot}56$, the directors at $z = \pm h$ will be in the first and fourth quadrants. On the other hand, when ϕ_0 is increased to say $1{\cdot}9$ radian, the directors at $z = \pm h$ will lie in the second and third quadrants. Taking into account the fact that the director field twists continuously from one plate to the other, it becomes clear that the net magnetic torque should change substantially under an increase in the twist.

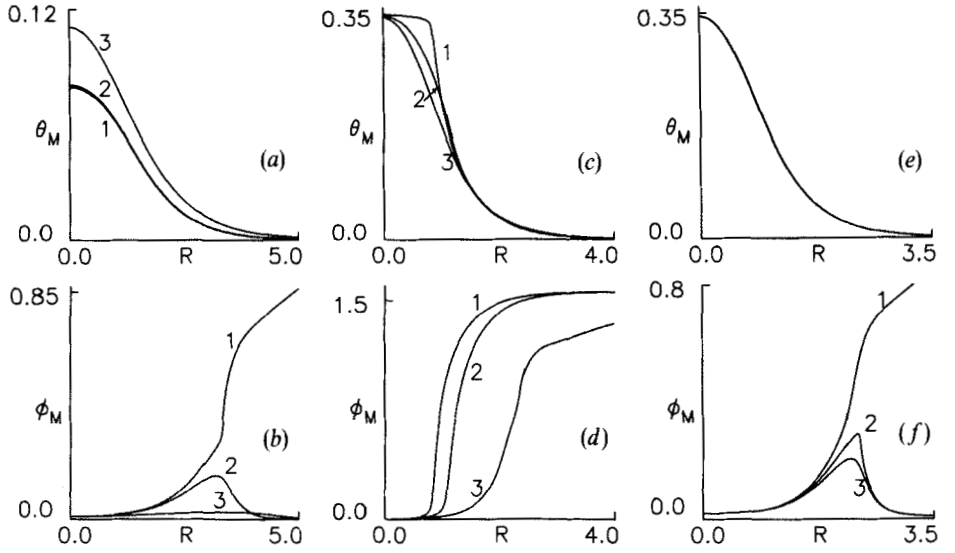

Figure 2. Plots of θ_M and ϕ_M as functions of reduced field R for $\alpha = 0$ and $\beta = 1{\cdot}56$ radian; **H** is applied in the xy plane and is close to the y axis. The ground state is S_1. (*a*) and (*b*) Parameters of E7 are utilized. The director pre-tilt at the sample planes is $\theta_0 = 0{\cdot}05$ radian. The overall twist is represented by $\phi_0 = (1)$ 1·58 (2) 1·6 (3) 1·95 radian. (*c*)–(*f*), 5CB parameters, $\theta_0 = 0{\cdot}35$ radian. In (*c*) and (*d*) curves as drawn ϕ_0 (1) 0·39 (2) 1·17 (3) 1·56 radian. Curve 3 shows a tendency towards a different behaviour. In (*e*) and (*f*) $\phi_0 = (1)$ 1·58 (2) 1·59 (3) 1·6. A small change in ϕ_0 close to β can produce a significant change in the qualitative nature of the variation of distortion with R (see § 3.2.).

3.3. *Variation of magnetic angles α and β*

Having determined the ranges of θ_0 and ϕ_0 over which a stable S_1 ground state exists, it is now possible to study the effect of changing the magnetic tilt at a given reduced field R; R is generally fixed at a modest value $\leqq 3$. Initially, β will be held constant and α will be changed. It appears sufficient to consider the range $0 \leqslant \alpha \leqslant \pi$. When $\beta \neq 0$ or π, the θ and ϕ profiles are non-symmetric but, as before, the distortion at the sample centre will be used for presenting the results. For reasons which will become clear, it is advisable to discuss separately the case of low twist ($\phi_0 < \pi/2$) and that of high twist ($\phi_0 \approx \pi/2$).

When ϕ_0 is sufficiently small (say 0·39, 0·78 or 1·17 radian) the variation of θ_M and ϕ_M with α is found to be very similar to that depicted in figure 4 of [18] and therefore diagrams have not been shown. The following features emerge, strongly similar to previous results:

(i) If R is small (typically, < 1), θ_M and ϕ_M are single valued functions of α at fixed ϕ_0 and magnetic azimuthal angle β; this can be called *Type A variation of deformation.*

(ii) When R is high enough (> 1) but β sufficiently low, the θ_M and ϕ_M curves break up into two distinct branches as α is varied from the two extremities of its range; these branches overlap over the *bistable region* near the centre of the α range; this can be called the *Type B variation of distortion.* The width of the overlap or bistable region (the bistability width) generally increases with R at given ϕ_0 and β. On varying α beyond the edge of one branch, a stable S_1

deformation is found only on the corresponding point of the other branch. A feature which manifests itself here as before (see figure 4 of [18]) is the difference in shapes of the two branches of the curve caused by the different extents of coupling of splay–bend with twist.

(iii) At given ϕ_0, when R and β are sufficiently high, the variation of deformation with α lies on two distinct continuous branches when α is varied from the two ends of its range, but the overlap now extends over the entire π range of α; in other words, the bistability width in now π. This can be called *Type C variation of distortion.*

The only qualitative dissimilarity is noticed when both ϕ_0 and β are high (say, $\phi_0 = 1{\cdot}17$; $\beta = 1{\cdot}36$ radian); it is found that the bistability width at $R = 1{\cdot}5$ is actually *higher* than that at $R = 2{\cdot}0$. This reversal in trend is a portent of certain qualitative changes which can be expected with a further increase in the ground state twist of S_1.

Figure 3 depicts plots of θ_M and ϕ_M as functions of α when the total twist of the S_1 is close to $\pi(\phi_0 = 1{\cdot}56$ radian); both E7 (figures 3 (*a*)–(*d*)) and 5CB figures 3 (*e*) and (*f*)) are represented with different director pre-tilts at the boundaries. It is seen (curves 1) that the distortion changes continuously with α when R is low enough. When the field is stronger (curves 2), the deformation change lies on two separate branches which do not overlap near the centre of the α range; this can be called *Type D variation of deformation.*

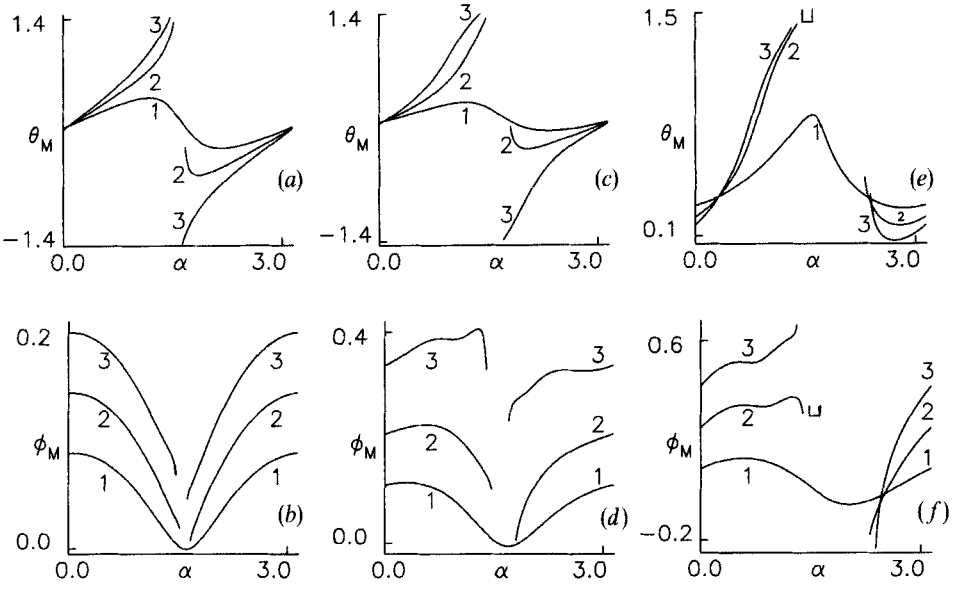

Figure 3. Variation of θ_M and ϕ_M with α, the magnetic polar angle at given values of β when the ground state twist is close to π ($\phi_0 = 1{\cdot}56$). In (*a*)–(*d*) the material parameters are those of E7 and the director pre-tilt at the boundaries $\theta_0 = 0{\cdot}05$; in (*e*) and (*f*) 5CB parameters have been used with $\theta_0 = 0{\cdot}35$ radian. The magnetic azimuthal angle β = (*a*) and (*b*) 0·39 (*c*)–(*f*) 1·17 radian. The following reduced field strengths have been employed. In (*a*)–(*d*) R = (1) 0·75 (2) 1·0 (3) 1·25. In (*e*) and (*f*) R = (1) 0·5 (2) 0·8 (3) 1·0. When R is sufficiently high, the two branches of a given curve fail to overlap near the centre of the α range, but leave a gap over which stable solutions of (5) satisfying (7) cannot be found. An irreversible transition from the edge of the gap to the corresponding state having lower overall twist (S_2 distortion) cannot be ruled out (see § 3.3.; also, compare with figures 6 (*a*) and (*b*)).

When α is changed in small steps near one edge of the gap on a given branch, a solution of (5) satisfying (7) cannot be found when α crosses the gap edge (the algorithm diverges). It thus appears that in these cases (curves 2, for instance) there may exist no solution satisfying (7) within the gap. We can now talk of a *gap width* in the case of Type *D* variation, just as we define a *bistability width* for Type *B* variation. The question that crops up now is, what happens in the gap? It will be seen presently (§ 3.4.) that an answer to this query may be found through linear perturbation analysis and energetics.

It should be made clear that the Type *D* variation of distortion has not so far been encountered in earlier work [14–18]. It should also be noted (see figures 3 (*a*) and (*c*), curves 1, 2) that a small change in the reduced field at a given β can considerably affect the shape of one of the branches of the θ_M curve. At this stage, an exact quantitative dependence of the gap width on R is not known. To ascertain this, it is necessary to make detailed calculations for a number of sets of parameters and this becomes time consuming. It is found, however, that the gap width increases with R at given ϕ_0 and β in some cases (see, for instance, figures 3 (*e*) and (*f*)).

The next task is to fix α at some value and vary β for different values of the reduced field R. Here again it is necessary to study separately the low twist and high twist regimes. Without loss of generality, the β range can be chosen to be $0 \leqslant \beta \leqslant \pi$.

When ϕ_0 is not close to π (say, $\phi_0 = 0{\cdot}39$, $0{\cdot}78$ or $1{\cdot}17$ radian) the variation of deformation with β is found to be qualitively similar to that given in figure 5 of [18]; hence the diagrams have not been included. The following points may, however, be noted:

(i) At given ϕ_0 and α, θ_M and ϕ_M are single valued functions of β when R is small (< 1); this is *Type A variation of distortion.*

(ii) When the field is stronger ($R > 1$), the θ_M and ϕ_M curves break up into two distinct branches when β is varied from 0 and from π (this is *Type B variation of deformation);* these branches overlap near the centre of the β range with the bistability width generally increasing with reduced field. When α is high enough, the two branches for the same R have different shapes; as before, this is interpreted as being due to the different extents to which the splay–bend and twist distortions couple when β is varied from the extremities of its range.

(iii) When α is sufficiently high, *Type C variation* is also noticed when the field is strong enough; this involves the deformation varying along two distinct branches which overlap over the entire β range.

These results should be contrasted with figures 4 (*d*)–(*f*) which have been obtained for a high twist of the S_1 ground state ($\phi_0 = 1{\cdot}56$ radian). It may be observed that at sufficiently elevated fields the two branches of the θ_M and ϕ_M curves fail to overlap near the centre of the β range leaving a gap where stable solutions of (5) satisfying (7) cannot be found (*Type D variation of distortion*). It is found (see figures 4 (*c*) and (*d*) drawn for E7 parameters) that this behaviour occurs even at low R when α is sufficiently high; in general, the gap width increases with field strength. The results for 5CB (see figures 4 (*e*) and (*f*)) are given for comparision.

Before closing this section, mention must be made that the above studies have also been extended to E7 parameters with a higher director pre-tilt of $\theta_0 = 0{\cdot}15$ radian. It is found that the qualitative nature of the results is unaffected; some of the effects are, however, accentuated. For instance, the gap width for α variation (β variation) becomes broader as compared to that for the corresponding case of lower director pre-tilt.

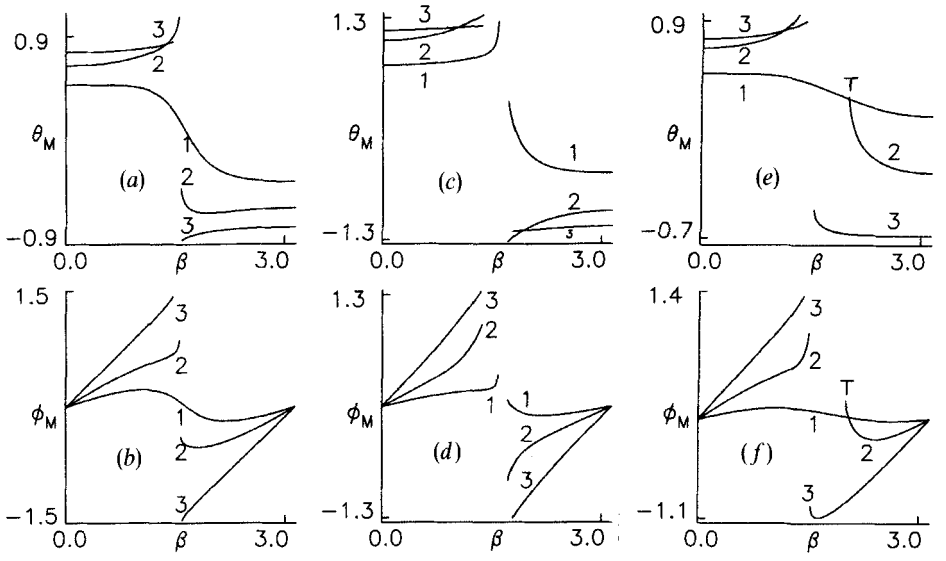

Figure 4. θ_M and ϕ_M versus β, the magnetic azimuthal angle for $\phi_0 = 1{\cdot}56$ (overall twist of S_1 is close to π radian). In (*a*)–(*d*) E7 parameters are used with $\theta_0 = 0{\cdot}05$ radian; in (*e*) and (*f*) 5CB parameters are employed with the director pre-tilt at the boundaries $\theta_0 = 0{\cdot}35$. The magnetic polar angle α = (*a*) and (*b*) 0·78, (*c*) and (*d*) 1·17, (*e*) and (*f*) 0·78 radian. The reduced field R takes the following values. R = (1) 1·0 (2) 1·5 (3) 3·0 in (*a*)–(*d*). R = (1) 0·5 (2) 1·0 (3) 2·0 in (*e*) and (*f*). When the field is sufficiently strong, it appears that stable solutions of (5) satisfying the boundary condition (7) may not exist in the gap near the centre of the β range. It seems reasonable to conclude (see figure 7 (*a*) and (*b*)) that there might occur a transition to the S_2 state having lower overall twist (see § 3.3.).

3.4. *Stability analysis of the S_1 deformation states*

As was done in earlier studies [17, 18], it is natural to wonder about the stability of the static distortions which are obtained by solving (5) with (7). This becomes particularly important when the deformation lies on two distinct branches which either overlap or do not (as in figures 3 and 4). It must be remembered that in the present work we are studying director profiles described by two angles, and it is necessary to use the time dependent stability analysis which was developed in [18]; a brief description of this technique is given below.

Consider the static distortion (3). It is now assumed that perturbations $\theta''(z, t)$ and $\phi''(z, t)$ are imposed, respectively, on $\theta(z)$ and $\phi(z)$; t is the time coordinate. Then the director field is given by

$$\mathbf{n}'' = [\cos(\theta + \theta'')\cos(\phi + \phi''),\ \cos(\theta + \theta'')\sin(\phi + \phi''),\ \sin(\theta + \theta'')]. \tag{14}$$

It should be noted that the perturbations are supposed to be dependent on only one spatial coordinate, z. According to continuum theory [1–5], the time rates of change of the director perturbations, $\partial\theta''/\partial t$ and $\partial\phi''/\partial t$ give rise to the viscous stress components Σ_{zx} and Σ_{zy}; these, in turn, bring into existence the velocity field

$$v = [v_x(z, t),\ v_y(z, t),\ 0], \tag{15}$$

which is also a function of z and time. As the director perturbations have been taken to be of first order, it is reasonable to regard the velocity components in (15) to be linear

perturbations. Linearizing with respect to the perturbations and their derivatives and using (5), one obtains a set of four coupled linear partial differential equations (see equations (4.8) of [18]) which are solved with the boundary conditions

$$\theta''(z=\pm h,t)=0; \quad \phi''(z=\pm h,t)=0; \quad v_x(z=\pm h,t)=0; \quad v_y(z=\pm h,t)=0; \quad (16)$$

these represent rigid anchoring of the director as well as the no-slip condition of the velocity at the sample planes. If the director anchoring is weak, the first and second conditions in (16) will have to be modified.

It is possible to separate out the variable t by using the ansatz $\exp(\nu t)$ for the time dependence of the perturbations; this reduces the governing equations to a set of linear coupled ordinary differential equations which can be solved with the boundary conditions (16) to evaluate ν, the inverse relaxation time at given values of the reduced field, magnetic tilt angles, ground state twist and boundary tilt; ν is found as an eigenvalue satisfying a compatibility condition (for details of solution, see § 4.2. of [18]). In general, many solutions can be found for ν and all of them satisfy the compatibility conditions. Out of these, only the least negative value, ν_G, is chosen; this corresponds to the least damped mode. It is now possible to study ν_G as a function of different quantities.

In the present calculation, the material parameters of 5CB [25] have been used. The values of the elastic constants have been summarized in (12). The viscosity coefficients are assumed to be ([25]; see also equation 4.13 of [18]),

$$(\mu_1,\mu_2,\mu_3,\mu_4,\mu_5,\mu_6)=(0{\cdot}0,\ -0{\cdot}0941,\ -0{\cdot}0045,\ 0{\cdot}0824,\ 0{\cdot}0569,\ -0{\cdot}0417)\ \text{Pas}. \quad (17)$$

It is well known that the relaxation time of perturbations depends strongly on the sample thickness; therefore a semi-sample thickness of $h=100\ \mu$m has been employed.

Figure 5 summarizes some of the relevant results on the variation of ν_G with the magnetic tilt. It is found (see figure 5 (*c*), curves 2; figure 5 (*d*), curve 1; figure 5 (*f*), curve 1) that ν_G remains negative over the entire range of angles when the static distortion variation is continuous with bistability (Type *C*) or without it (Type *A*). When the static deformation exhibits bistability involving discontinuous changes (Type *B* variation; for instance, figure 5 (*c*), curves 1; figure 5 (*e*), curves 1), $\nu_G \to 0$ near the edges of the bistable region showing that the static distortion has the propensity to undergo instability at those points. A similar result is found to be valid in those cases (Type *D* variation) where a gap exists instead of the bistable region (figure 5 (*d*), curves 2; figure 5 (*f*), curves 2); as can be seen, $\nu_G \to 0$ when the magnetic angle approaches the edges of the gap.

Figure 5 (*a*) is relevant to figure 1 (*d*) (**H** applied normal to the sample planes) and shows that the deformation becomes unstable when the field strength is increased beyond a certain limit.

Results in figure 5 (*b*) should be compared with those in figure 1 (*b*). It is found that the static dostortion remains stable over the entire range of the ground state twist when $\theta_0=0{\cdot}35$ radian (curve 1); when $\theta_0=0{\cdot}37$ radian, however, instability sets in (curve 2) when ϕ_0 exceeds some threshold value ϕ_C. A noticeable feature of figure 5 (*b*) is the cusp which occurs on both curves. In this case, the ground state director orientation is such that θ is symmetric and ϕ antisymmetric with respect to the sample centre. It is natural that two distinct, uncoupled perturbation modes will exist, each mode having its own spatial symmetry. Such modes have been studied in a different context [27] and their time constants are known to cross over with variation of parameters. Remembering that ν_G is the least negative value of ν, it seems plausible that the cusp represents a point of cross over between two independent uncoupled perturbation modes.

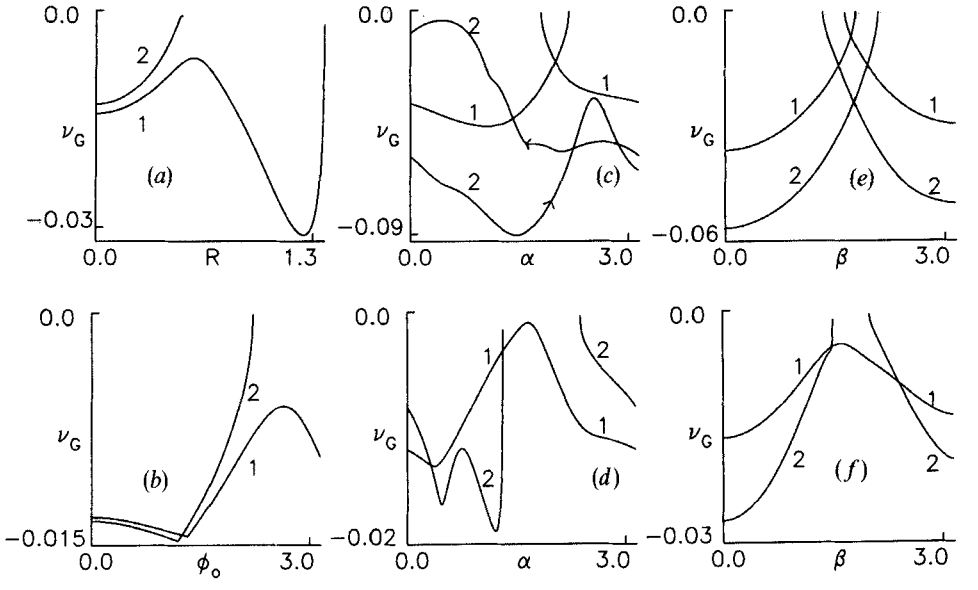

Figure 5. Results of linear stability analysis indicating variation of ν_G, the least negative value of the time constant, with different parameters. The material parameters are those of 5CB (12, 17). The sample thickness, $2h = 200\,\mu m$. (*a*) ν_G versus R, the reduced field, when **H** is normal to the sample planes; magnetic polar angle, $\alpha = 1{\cdot}57$. The director pre-tilt at the boundaries, $\theta_0 = 00{\cdot}35$ radian; For the the S_1 ground state, $\phi_0 = (1)\ 1{\cdot}36\ (2)\ 1{\cdot}56$. Compare with curves 2 and 3 of figure 1 (*d*). (*b*) ν_G versus ϕ_0 in the absence of the field; $R = 0$. $\theta_0 = (1)$ 0·35 (2) 0·37 radian. Compare with curves 1 and 2 of figure 1 (*b*). (*c*) ν_G as a function of α. $\theta_0 = 0{\cdot}35$; $\phi_0 = 0{\cdot}78$ radian. (1) $R = 1{\cdot}25$; $\beta = 0{\cdot}39$ radian (2) $R = 1{\cdot}9$; $\beta = 1{\cdot}17$. The arrows indicate the direction of change of α on the two curves for Type *C* variation of distortion (see figure 4 of [18] for illustrative plots of deformation). (*d*) Variation of ν_G with α for $\beta = 1{\cdot}17$, $\theta_0 = 0{\cdot}35$ and $\phi_0 = 1{\cdot}56$ radian. $R = (1)\ 0{\cdot}6\ (2)\ 1{\cdot}0$ (compare with figures 3 (*e*) and (*f*). (*e*) Plots of ν_G versus β. $\alpha = 0{\cdot}39$, $\theta_0 = 0{\cdot}35$ and $\phi_0 = 78$ radian. Results represent $R = (1)\ 1{\cdot}1$ (2) 1·5, (for illustrative plots of distortion, see figure 5 of [18]). (*f*) ν_G versus β for $\alpha = 0{\cdot}78$, $\theta_0 = 0{\cdot}35$ and $\phi_0 = 1{\cdot}56$ radian. $R = (1)\ 0{\cdot}7\ (2)\ 1{\cdot}0$, (compare with figures 4 (*e*) and (*f*), (see § 3.4.).

Before closing the discussion, it is worth noting that for Type *C* variation (see, for instance, figure 5 (*c*), curves 2) the value of ν_G is, in general, different for the two continuous branches of the deformation which are obtained by changing α from the two extremities of the range (the direction of α variation is indicated by the arrows). This also shows that the two states have, in general, different free energies at any given α. As described earlier [18], this seems to be caused by the different extents to which the fundamental deformations of a nematic couple with one another when the magnetic tilt is varied in opposite directions, interestingly, ν_G is negative for either branch which means that the distortions on both branches are stable against small perturbations. At the two extremities of the range, however, the time constant for one branch is higher than that of the other; essentially, the deformation at the end of one branch is *more stable* than that on the other branch. The question that arises is whether the distortion with higher ν_G is *more unstable* against non-linear perturbations. It should be instructive to find out what happens in this case when α is varied back and forth over its entire range of values.

4. Possible directions of change at gap edges

4.1. *Alternative deformation states*

The results of §3.4. have shown that the S_1 static distortion (3) satisfying the boundary conditions (7) becomes unstable against linear perturbations at certain values of field strength and tilt. The linear stability problem being one of the eigenvalue kind, the eigenvectors (actual magnitudes of the perturbations at threshold) are not completely determined; the actual direction of change at an instability is not known. In principle, this can be ascertained by a rigorous solution of the non-linear dynamical equations (see equations (4.3), (4.4) of [18]), but this task is beyond the scope of the present work. An attempt can still be made to understand the kind of end state the deformation acquires after undergoing instability by using previous results [11, 12] which are based on considerations of energetics and symmetry.

The first observation to be made is that before and after the instability, the orientation of the director field at the sample plates should remain unaltered; this is required by the rigid anchoring hypothesis. It is meaningful, at this stage, to understand this 'direction of orientation', not in terms of values assumed by angles, but in terms of a physical direction which is fixed relative to the chosen coordinate axes. But the non-polarity of the director field enables us to consider related states of deformation which may be obtainable by reversing the orientation of **n** at one of the plates without changing its physical direction.

To understand this, consider the ϕ_0 variation at $\theta_0 = 0{\cdot}05$ radian in the absence of a magnetic field (figure 1 (*a*), curve 1). When $\phi_0 = \pi/2$, the S_1 ground state has a total twist of $2\phi_0 = \pi$(this is also referred to as a $\mathscr{T}$ *state* in [11, 12]). While the director at the sample centre is along the x axis, the directors at the boundaries are in the yz plane such that

$$\mathbf{n}(z = \pm h) = (0, \pm\cos\theta_0, \sin\theta_0). \tag{18}$$

This is a distortion having $\theta(z)$ symmetric and $\phi(z)$ antisymmetric. It is immediately clear that if we could reverse the *direction* of **n** at one of the plates (say, at $z = -h$), we could get a different deformation state in which the director orientation at the two plates is still in the yz plane, but given by

$$\mathbf{n}(z = \pm h) = (0, \cos\theta_0, \pm\sin\theta_0), \tag{19}$$

with an overall twist of only $2\phi_0 - \pi = 0$; in this state, $\theta(z)$ is antisymmetric and this state can be identified with the $\mathscr{H}$ *state* in [11, 12].

The above considerations enable us to study a related ground state (which we shall refer to as S_2) which is given by the distortion (3) but with the boundary conditions

$$\theta_\pm = \pm\theta_0; \qquad \phi_- = \pi - \phi_0; \qquad \phi_+ = \phi_0. \tag{20}$$

In the particular case of $\phi_0 = \pi/2$, this reduces to the $\mathscr{H}$ *state*. For general values of θ_0 and ϕ_0, the S_2 ground state is associated with angles $\theta(z)$ and $\phi(z)$ such that $\theta(z)$ and $\phi(z) - \pi/2$ are both antisymmetric. Thus the S_2 ground state can be regarded as a generalization of the $\mathscr{H}$ *state* by the imposition of an overall twist of $2\phi_0 - \pi$. In the present description of the S_2 ground state, the director at the sample centre will lie along the y axis.

It is clear that the S_1 and S_2 ground states are *topologically inequivalent* [11]; there exists no continuous transformation which can take the S_1 distortion into the S_2 deformation or vice versa. It need hardly be emphasized that the governing equations (5) can be solved with the boundary conditions (20) to yield the $\theta(z)$ and $\phi(z)$

profiles corresponding to the S_2 state. When the magnetic field is impressed along some arbitrary direction, it is unlikely that $\theta(z)$ and $\phi(z)$ will exhibit the symmetries of the S_2 ground state. Still, using the same convention as before, we shall refer to any static distortion obtained by solving the governing equations (5) with the boundary conditions (20) as the S_2 deformation.

Consider, for instance, curve 1 of figure 1 (*a*). When $\phi_0 > \phi_C \approx 2{\cdot}35$ radian, the S_1 ground state cannot exist. A comparison of the total free energies of the S_1 and S_2 states in the absence of an external field shows that at $\phi_0 \approx \phi_C$, S_2 has much lower free energy than S_1; the reason is that the S_2 ground state is associated with a much lower overall twist (about 1·6 radian) than the S_1 ground state (4·7 radian). This enables us, along with the results of § 3.4., to put forward the hypothesis that when ϕ_0 exceeds ϕ_C, a transition should take the deformation from the S_1 kind to the S_2 kind. When such a transition occurs, the excess of free energy will be dissipated by viscous effects; in addition, the overall twist will be reduced considerably (by nearly π radians). Hence, the transition is likely to be irreversible.

4.2. *Results for the solution* S_2

With the above discussion, it is now possible to continue the study of figures 3 and 4 which represent the variation of S_1 deformation as a function of the magnetic tilt, the overall twist being $2\phi_0 = 3{\cdot}12$ radians. This is done by comparing the above results with those obtained for the S_2 solution with the same value of ϕ_0 (total twist being about 0·02 radian). In order that the field strength might remain unchanged, the same definition (10) is used for the reduced field R. It should be borne in mind that the S_2 ground state is obtained by starting with a reversely pre-tilted splay–bend distortion in the yz plane and imparting to it an overall twist of $2\phi_0 - \pi$. When this is done, the director at the sample centre will lie along the y axis ($\phi = \pi/2$ and $\theta = 0$) with equal and opposite twists of magnitudes $|\phi_0 - \pi/2|$ on either side of the sample centre.

Figure 6 shows plots of θ_M and ϕ_M as functions of α, the magnetic polar angle. In figures 6 (*a*) and (*b*), the values of R and β used are the same as those employed in figures 3 (*e*) and (*f*). It is found that either the deformation varies continuously over the entire α range without exhibiting bistability (Type A variation) or it lies on two branches which overlap near the centre of the α range (Type B variation); in either case, there are no gap widths as in figures 3 (*e*) and (*f*). It is, therefore, possible that when the solution S_1 becomes unstable (see, for instance, the points U on curves 2, figures 3 (*e*) and (*f*)) at one edge of the gap, a transition occurs to the corresponding points U (figures 6 (*a*) and (*b*); curve 2) so that the distortion changes over to the S_2 type. When α is varied further, the deformation will remain of the S_2 type and will lie on curve 2 of figures 6 (*a*) and (*b*). The transition from S_1 to S_2 is likely to be irreversible. A similar conclusion can be arrived at by comparing the curves 3 in the same set of diagrams. Under the transition $S_1 \rightarrow S_2$, the total twist in the sample gets reduced by nearly π radian. It is also clear now that if the field strength is gradually reduced to zero, the S_2 and not the S_1 ground state results.

While figures 6 (*a*) and (*b*) deal with a low overall twist of the S_2 distortion, figures 6 (*c*)–(*f*) describe the variation of the S_2 deformation with α at higher ground state twist. Of particular interest are figures 6 (*e*) and (*f*) which are drawn for $\phi_0 = 0$ (overall twist = π radians); in this case, the directors at the sample boundaries will lie in the xz plane. It is found that at sufficiently elevated fields there are gaps in the α range over which the S_2 distortion satisfying boundary conditions (20) may not exist. By using the same arguments that were employed in § 4.1., it can be concluded that when α

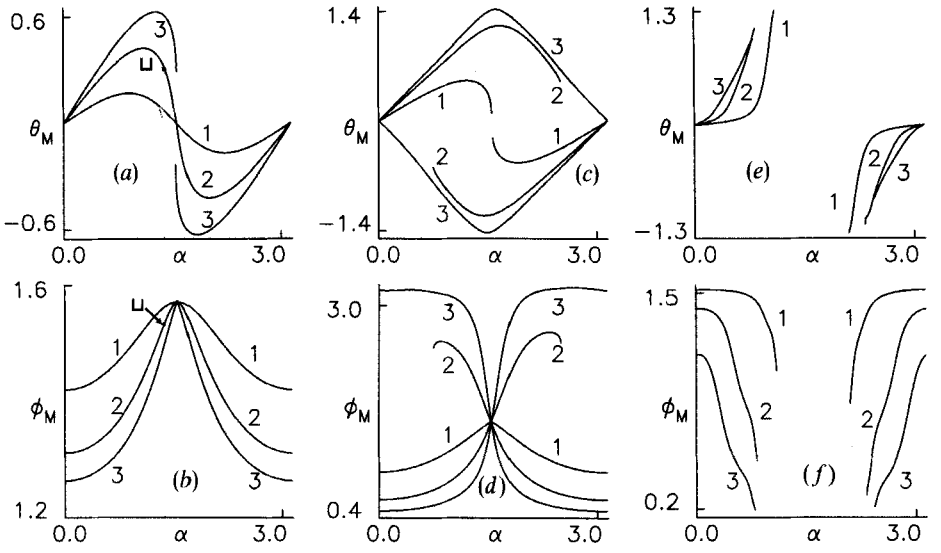

Figure 6. Variation of deformation with the magnetic polar angle α for different values of the magnetic aximuthal angle β and reduced field R. The ground state which is of type S_2 (20) is in a reversely pre-tilted cell and on it a twist of $2\phi_0 - \pi$ is imposed. In (*a*) and (*b*), 5CB parameters are used with $\phi_0 = 1{\cdot}56$, $\beta = 1{\cdot}17$ and $\theta_0 = 0{\cdot}35$ radian. $R = (1)\ 0{\cdot}5\ (2)\ 0{\cdot}8\ (3)\ 1{\cdot}0$. An irreversible change from S_1 (see figures 3 (*e*) and (*f*)), to S_2 may occur at U; after the change-over, the distortion will continue to be S_2 as there results considerable diminution in the twist. In figures (*c*)–(*f*), E7 parameters have been chosen with $\theta_0 = 0{\cdot}05$ radian. The reduced field $R = (1)\ 1{\cdot}0\ (2)\ 1{\cdot}5\ (3)\ 2{\cdot}0$. The remaining quantities take the following values: (*c*) and (*d*) $\phi_0 = 0{\cdot}78$; $\beta = 0{\cdot}39$ (*e*) and (*f*) $\phi_0 = 0{\cdot}0$; $\beta = 0{\cdot}05$ radian. It is seen from (*e*) and (*f*) that when the overall twist of the S_2 deformation is high enough, a suitably directed magnetic field may cause an irreversible change in the distortion of the S_1 kind when α crosses the edges of the gap, greatly reducing the total twist in the sample (§ 4.2.).

varies beyond the gap edges, the deformation changes from the S_2 type to the S_1 type (13) satisfying boundary conditions (7) and having an overall zero twist. This appears to indicate that an irreversible transition from S_2 to S_1 is also possible under certain conditions.

The variation of the magnetic azimuthal angle offers a somewhat greater variety keeping in mind the nature of the S_2 ground state. Figures 7 (*a*) and (*b*) depict plots of the deformation versus β at different values of reduced field for 5CB parameters at $\phi_0 = 1{\cdot}56$; the director pre-tilt $\theta_0 = 0{\cdot}35$ and $\alpha = 0{\cdot}78$ radian. The β range is the same as that used in figure 4. It is found that θ_M and ϕ_M are single valued and continuous over the entire β range (Type A variation). Curves drawn for E7 parameters with $\theta_0 = 0{\cdot}05$ and different values of ϕ_0 ($= 0{\cdot}39, 0{\cdot}78, 1{\cdot}17$) have essentially the same shape as those of figures 7 (*a*) and (*b*); these results have not been presented. Comparing figures 7 (*a*) and (*b*) with figures 4 (*e*) and (*f*) it becomes clear that transitions from the points T at the gap edges in figures 4 (*e*) and (*f*) to the corresponding points in figures 7 (*a*) and (*b*) may be expected; again, such a transformation can be understood to be irreversible.

For the S_2 ground state (20), one can consider a second range for β variation, namely, $\pi/2 \leqslant \beta \leqslant 3\pi/2$. Figures 7 (*c*)–(*f*) show the nature of deformation change with β for E7. In figures 7 (*c*) and (*d*), the total twist in the sample is small ($\phi_0 = 1{\cdot}56$). It is possible to discern all three types (A, B, C) of variation for different field strengths.

In figures 7 (*e*) and (*f*), the overall twist is nearly π radian ($\phi_0 = 0$). When the field is weak (curves 1), the distortion change is of Type *A*–i.e. single valued and continuous over the entire β range. At more elevated field strength (curves 2) it appears that a solution of the governing equations satisfying boundary conditions (20) cannot be found over the gap width near the centre of the β range. As conjectured earlier, it is likely that when β crosses the gap edges, the S_2 deformation changes over irreversibly and discontinuously to a distortion of the S_1 kind having much lower total twist ($=0$) and satisfying the conditions (7). The argument can be given exactly as it was in § 4.1. The diagrams for the S_1 solution at $\phi_0 = 0$ and corresponding field strengths have not been provided for comparison. Obviously, the variation of S_1 distortion will be of Types *A*, *B* or *C* and once the change over has occurred (the ground state will be of the kind studied in [18]) from S_2, the deformation will continue to remain S_1.

It may be noted (see figures 7 (*a*) and (*b*)) that there exists a qualitative difference between the low field (curves 1) and high field regimes (curves 2 and 3). The S_2 ground state (20) is one in which $\theta_M = 0$, $\phi_M = \pi/2$, corresponding to antisymmetry of $\theta(z)$ and $\phi(z) - \pi/2$. When the field is low (curves 1), $\theta_M \to 0$ and $\phi_M \to \pi/2$ at either end of the β range, $0 \leqslant \beta \leqslant \pi$ and the S_2 deformation assumes the symmetries of the S_2 ground state at the two extremities of the β range when the field is not very strong; for other values of β, the distortion becomes non-symmetric. When $\beta = 0$ or π, **H** lies in the *xz* plane and is normal to the ground state director field at $z = 0$. Thus when the field is weak, the director at the sample centre assumes the *y* direction when $\beta = 0$ or π *even in the presence of a field.*

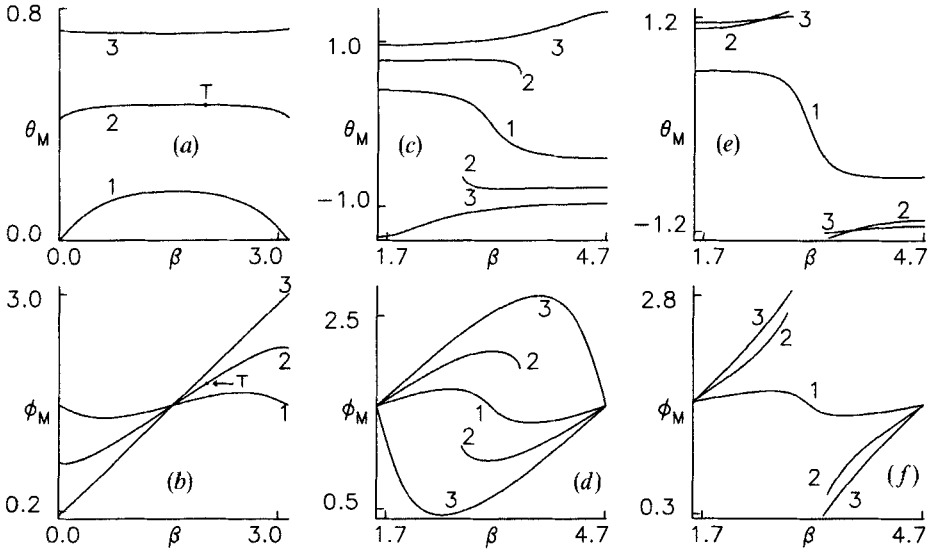

Figure 7. Plots of θ_M and ϕ_M as functions of β for different values of α and R. The ground state is S_2 (20) with the total twist in the sample being $\pi - 2\phi_0$. (*a*) and (*b*) $\phi_0 = 1{\cdot}56$. 5CB parameters. $\theta_0 = 0{\cdot}35$. $\alpha = 0{\cdot}78$. $R = (1)\ 0{\cdot}5\ (2)\ 1{\cdot}0\ (3)\ 2{\cdot}0$. The β range $0 \leqslant \beta \leqslant \pi$ which is the same as that employed in figure 4. T is the point of an irreversible transition from S_1 (see figures 4 (*e*) and (*f*) to S_2. (*c*)–(*f*) The β range is $\pi/2 \leqslant \beta \leqslant 3\pi/2$. E7 parameters. $\theta_0 = 0{\cdot}05$. $\alpha = 1{\cdot}17$. (*c*) and (*d*) $\phi_0 = 1{\cdot}56$. The curves are represented by $R = (1)\ 1{\cdot}0\ (2)\ 1{\cdot}5\ (3)\ 2{\cdot}0$. (*e*) and (*f*) $\phi_0 = 0{\cdot}0$. The curves are drawn for $R = (1)\ 0{\cdot}8\ (2)\ 1{\cdot}5\ (3)\ 2{\cdot}2$. When β approaches the edges of the gap near the centre of the range and the overall twist is sufficiently high, the deformation may change from the S_2 *to the* S_1 type (see § 4.2.).

When the field is strong enough, however, θ_M remains non-zero over the entire β range; in addition, the ϕ_M at the extremities of the β range differ considerably from $\pi/2$ and the distortion will remain non-symmetric over the entire β range. This leads to the following conclusion. Let $\beta=0$ or π; let α also take some value. We start with the S_2 ground state (20) and increase H gradually. Initially, $\theta(z)$ and $\phi(z)-\pi/2$ will remain antisymmetric (calculations show that this is, indeed, true; the $\theta(z)$ and $\phi(z)$ profiles do get deformed under an increase of field, but they retain the symmetries of the S_2 ground state). When H exceeds some critical threshold H_C, a transition occurs and the director distortion becomes asymmetric. This view is especially strengthened by the realization that **H**, which lies in the xz plane, does not exert any torque on the director (oriented along the y axis) at the sample centre of the S_2 ground state. An increase of H causes a build up of distortion on either side of the sample centre. When the field is strong enough, this deformation may be so great that a stable solution satisfying (20) may not be possible if it also has to satisfy the symmetires of the S_2 ground state and a transition occurs to a non-symmetric distortion state. Such transitions have been studied earlier [28] for special orientations of electric and magnetic fields.

Assuming that such a transition is possible (presently, we prove that it exists), the following questions arise:

(i) At the threshold, will small perturbations in the director field tend to grow?
(ii) Will the transition be of first order or second order?
(iii) Will domains form above the threshold?

An attempt is made to answer the first two questions in the next section. It is rather difficult to answer the last one, as the deformation has been assumed to depend on only one coordinate in the present work. It is also clear from figures 7 (*a*) and (*b*) that when the field is strong enough, ϕ_M appears to take a low value when β is zero and assumes a high value at the other end of the β range. In addition, the variation of distortion is seen to be single valued (it is of Type *A*, rather than of Type *C*). It seems, therefore, that when β is close to zero (or π), ϕ_M will be nearer zero (or π) at high field strengths. Hence, one domain at a time will be considered in the present work depending upon the value of β.

4.3. *Estimation of the threshold H_C at $\beta=0$, π*

Before setting up the governing equations for linear perturbations, it seems worth studying the variation of S_2 deformation (20) as a function of the field strength at the two ends of the β range. For this section alone, we use

$$r=H/H_S; \qquad H_S=(\pi/2h)(K_1/\mu_0\chi_A) \tag{21}$$

to represent the reduced field where H_S is the splay Fréedericksz threshold; H_F (9) is ϕ_0 dependent and we have to compare curves for different ϕ_0 in the same diagram. Figures 8 (*a*)–(*f*) summarize the salient results. It is convenient to discuss the results under two broad categories—results for low overall twist (see figures 8 (*a*)–(*d*)) and those for high twist (see figures 8 (*e*) and (*f*)).

It is observed (see figures 8 (*a*)–(*d*)) that for fixed α (magnetic polar angle) and boundary tilt (θ_0), $\theta_M\neq 0$ and $\phi_M\neq\pi/2$ when r is sufficiently high. When r is diminished and $r\rightarrow$some threshold r_C, it is found that $\theta_M\rightarrow 0$ and $\phi_M\rightarrow\pi/2$; for $r<r_C$, θ_M and ϕ_M maintain their constant values (this results in horizontal straight lines in the diagrams; these parts of the diagrams have not been plotted to avoid conflict between different curves). It is clear from these diagrams that the transition is one of second order. Another feature that emerges is that for $\beta=0$ and $\beta=\pi$, the θ_M curves practically

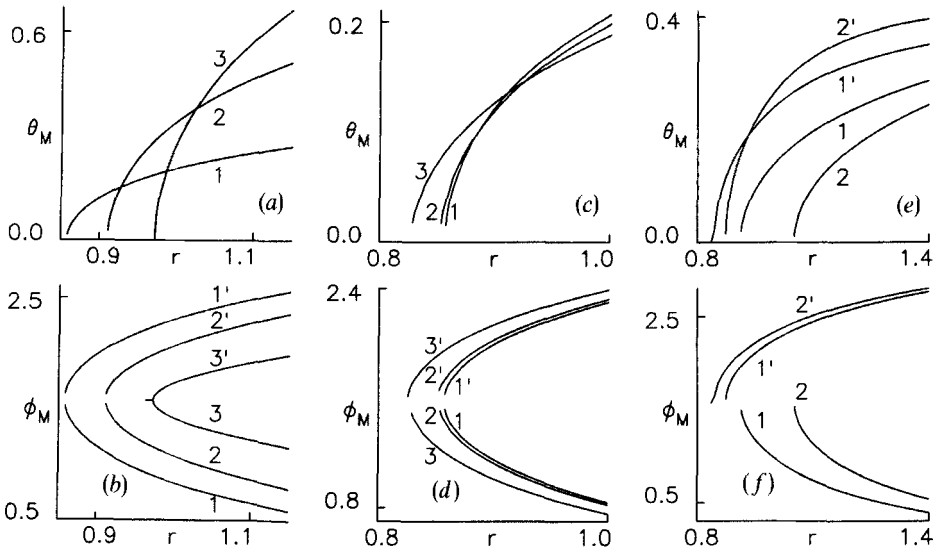

Figure 8. Variation of S_2 deformation with magnetic field strength for different values of the director boundary tilt (θ_0), magnetic polar angle α and ϕ_0 (overall imposed twist $\pi - 2\phi_0$). E7 parameters have been employed. The curves with primed (unprimed) numbers are drawn for $\beta = \pi$ ($\beta = 0$). The dimensionless field $r = H/H_S$ where H_S is the splay Fréedericksz threshold. In (*a*)–(*d*), the θ_M curves nearly coincide for $\beta = 0$ and $\beta = \pi$. (*a*) and (*b*) $\phi_0 = 1{\cdot}56$, $\theta_0 = 0{\cdot}05$, $\alpha = (1)\ 0{\cdot}4\ (2)\ 0{\cdot}8\ (3)\ 1{\cdot}2$, (*c*) and (*d*) $\phi_0 = 1{\cdot}56$, $\alpha = 0{\cdot}4$, $\theta_0 = (1)\ 0{\cdot}05\ (2)\ 0{\cdot}45\ (3)\ 0{\cdot}75$, (*e*) and (*f*) $\theta_0 = 0{\cdot}45$, $\alpha = 0{\cdot}4$, $\phi_0 = (1)\ 1{\cdot}17\ (2)\ 0{\cdot}78$. When $r >$ a threshold r_C, the distortion becomes non-symmetric. If the imposed twist is small enough ((*a*)–(*d*)), r_C for $\beta = 0$ and $\beta = \pi$ coincides for different values of α and θ_0. The two thresholds become different when the total twist is enhanced (figures (*e*) and (*f*); see §4.3.).

coincide. The ϕ_M curves, however, lie on two distinct branches, but both branches approach the value of $\pi/2$ at almost the same r_C value. Predictably, at a fixed θ_0 (see figures 8(*a*) and (*b*)), r_C increases with α; for a given α (see figures 8(*c*) and (*d*)), r_C diminishes when the boundary tilt is enhanced.

In figures 8(*e*) and (*f*), a fairly high boundary tilt ($\theta_0 = 0{\cdot}45$) has been chosen. The magnetic polar angle has also been fixed sufficiently away from zero ($\alpha = 0{\cdot}4$); this means that the directions of **H** for the two β values will not coincide. The results have been presented for two fairly elevated values of the overall twist ($\phi_0 = 0{\cdot}78$, $1{\cdot}17$ radian; equivalently, the total twist is approximately $\pi/2$, $3\pi/4$, respectively). While the shapes of the curves are similar to those in figures 8(*a*)–(*d*), one important deviation is discernible. For a given ϕ_0, the r_C value for $\beta = 0$ and that for $\beta = \pi$ do not match; in general, the former seems to be higher than the latter. Calculations have shown (results have not been presented here) that r_C becomes identical for $\beta = 0$ and π when the magnetic polar angle, α, is zero for the same high values of ϕ_0 and θ_0; in this case, **H** would be directed along the x axis for both values of β. It is now required to calculate r_C for different parameters.

It is possible, in principle, to employ the time dependent perturbation technique (as in §3.4) to determine r_C. One can guess that for $r < r_C$, the time constant $\nu_G < 0$; when $r \to r_C$, $\nu_G \to 0$. It is, however, much simpler to use the time independent perturbation technique to determine the threshold r_C. In this method it is sufficient to consider

perturbations only on the director field neglecting time dependence and the associated viscous effects. The perturbations $\theta''(z)$ and $\phi''(z)$ imposed on $\theta(z)$ and $\phi(z)$, respectively, are assumed to be functions of z alone so that the resulting director field takes the form (14). Using the torque equations (5) satisfied by $\theta(z)$ and $\phi(z)$, the governing equations for the perturbations can be written as

$$\left.\begin{aligned} &f_2(\theta)\theta''_{,zz}+[(df_2/d\theta)\theta_{,z}]\theta''_{,z}-\phi''_{,z}[(df_3/d\theta)\phi_{,z}]-\phi''(\partial^2 f_4/\partial\theta\partial\phi)\\ &+\theta''[df_2/d\theta)\theta_{,zz}+\tfrac{1}{2}(d^2 f_2/d\theta^2)\theta^2_{,z}-\tfrac{1}{2}(d^2 f_3/d\theta^2)\phi^2_{,z}-(\partial^2 f_4/\partial\theta^2)]=0;\\ &\theta''_{,z}[(df_3/d\theta)\phi_{,z}]+f_3(\theta)\phi''_{,zz}+\phi''_{,z}[(df_3/d\theta)\theta_{,z}]-(\partial^2 f_4/\partial\phi^2)\phi''\\ &+\theta''[(df_3/d\theta)\phi_{,zz}+(d^2 f_3/d\theta^2)\theta_{,z}\phi_{,z}-(\partial^2 f_4/\partial\theta\partial\theta)]=0. \end{aligned}\right\} \quad (22)$$

The boundary conditions for the perturbations under the rigid anchoring hypothesis become

$$\theta''(z=\pm h)=\phi''(z=\pm h)=0. \quad (23)$$

The orthogonal collocation method [22] can be conveniently employed to solve relations (22) and (23). Clearly, this becomes an eigenvalue problem from which the critical value of r can be determined; the absolute magnitudes of the eigenvectors (the perturbation profiles) remain unknown. The method of solution is as follows. First, β is fixed at zero. Then, at given values of θ_0, ϕ_0 and α, the S_2 deformation is calculated by solving (5) with (20) taking zero field strength and the compatibility condition resulting from the eigenvalue problem (22) and (23) are evaluated. This is repeated by increasing H in small steps until, at a certain critical value H_C the compatibility condition is satisfied. This defines r_C for the given case. By varying different parameters, the variation of r_C is studied for $\beta=0$. Needless to say, the entire procedure can be repeated for $\beta=\pi$. The critical field determined in this way is found to be close to that shown in figure 8.

Plots of r_C versus θ_0 are found in figure 9 for two widely differing values of overall twist; E7 parameters have been used. The following conclusions can be reached. In all cases r_C is identical for $\beta=0$ and $\beta=\pi$ when θ_0 is sufficiently small. In particular, the r_C versus, θ_0 curves are practically identical (see figures 9 (*a*) and (*b*)) for the two β values when the overall twist $(\pi-2\phi_0)$ is not high. When ϕ_0 is low (see figures 9 (*c*)–(*f*)), the r_C versus θ_0 curves at $\beta=0$ and π are similar in shape only for α close to zero (for instance, curves 1). When α is sufficiently elevated, however, the variation of r_C with θ_0 is found to be quite different for $\beta=0$ and π. For instance, when θ_0 is sufficiently high (say, 0·4 radian), r_C at $\beta=0$ is found to be higher than that at $\beta=\pi$; this is in qualitative agreement with the results of figure 8. When α is increased close to $\pi/2$, it is expected that the curves for $\beta=0$ and π should again become similar in shape; this is mainly because at $\alpha=\pi/2$, when **H** is normal to the sample planes, β becomes irrelevant. This is, indeed, found to happen (curves 2 in figures 9 (*e*) and (*f*)).

It is rather predictable that in all cases, $r_C\to 0$ as $\theta_0\to\pi/2$. It is worth discussing this point in two stages. Firstly, let us assume that the S_2 ground state exists for any value of θ_0. Then the elastic deformation energy of the ground state would become considerable for θ_0 close to $\pi/2$ (remembering that $\theta(z)$ is antisymmetrical) and an instability could set in at very low field strengths. This takes us to the next question: In a real situation, is it possible to have the S_2 ground state with high pretilt angles θ_0?

To obtain the S_2 ground state one prepares a reversely pre-tilted sample (19) with no overall twist with a director pre-tilt of θ_0 at the boundaries. At this stage one expects

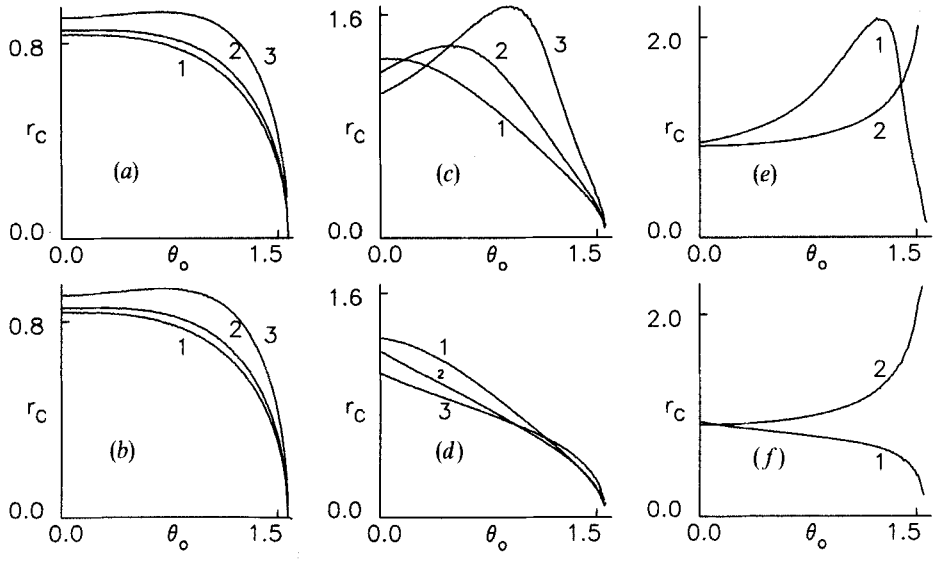

Figure 9. Plots of r_C versus θ_0, the director pre-tilt at the sample boundaries for different values of ϕ_0 and α. The parameters of E7 have been used, **H** is applied in the xz plane with $\beta = 0$ (*a*), (*c*) and (*e*) or $\beta = \pi$ (*b*), (*d*) and (*f*). The deformation is of S_2 type (20) such that $\theta(z)$ and $\phi(z) - \pi/2$ are antisymmetric relative to the sample centre as long as r, the reduced field (defined as in figure 8) is less than the critical value r_C. Above r_C, the distortion becomes non-symmetric. The overall twist is $\pi - 2\phi_0$ with $\phi_0 =$ (*a*) and (*b*) 1·56 (*c*)–(*f*) 0·39 radian. The magnetic polar angle $\alpha =$ (1) 0·05 (2) 0·39 (3) 0·78 in (*a*)–(*d*); $\alpha =$ (1) 1·17 (2) $\pi/2$ in (*e*) and (*f*). For small overall twist (*a*) and (*b*) the curves are identical at both β values (*a*) and (*b*). When the overall twist is high enough (*c*)–(*f*) the two curves become dissimilar in shape especially for $\alpha = 0{\cdot}78$, 1·17; the shape similarity is regained for $\alpha = \pi/2$ (*e*) and (*f*), curves 2. Parts of the curves in the high θ_0 range may not be of practical interest (see § 4.3.).

a mono-domain splay–bend distortion with $\theta(z)$ being antisymmetric; when θ_0 is low enough, this would correspond to the $\mathscr{H}$ *state* described in [11, 12]. The S_2 ground state now results when the two sample planes are twisted in opposite directions about the z axis through the same angle $|\pi/2 - \phi_0|$. But it is well known [11, 12] that when θ_0 is high (typically, $\theta_0 > \pi/4$), it is not possible to get the $\mathscr{H}$ *state* alone; the sample generally breaks up into adjacent domains of $\mathscr{H}$ and $\mathscr{V}$ *state* separated by 180° twist walls. It is not clear, for example, as to what will happen if, on such a sample, a non-trivial overall twist (of say $\pi/4$) is imposed; will a mono-domain S_2 ground state result through annihilation of defects? An answer can be provided by experiment. For the moment, it is advisable to consider portions of the r_C versus θ_0 curves (see figure 9) in the high θ_0 range to be only of academic interest.

Before closing this section, it seems worth commenting on the special case of $\phi_0 = \pi/2$ (the ground state is the $\mathscr{H}$ *state* in which ϕ is a constant and $\theta(z)$ is antisymmetric). When $\alpha \neq 0$, the results are similar to those for the S_2 case with low overall twist ($\phi_0 = 1{\cdot}56$); when $r < r_C$, $\theta(z)$ is antisymmetric and $\phi(z) = \pi/2$; when $r > r_C$, both $\theta(z)$ and $\phi(z)$ become non-symmetric in the sample. In the particular case of $\alpha = 0$ (**H** lies along the x axis for both $\beta = 0$ and π), however, the distortion above threshold is one in which $\theta(z)$ is antisymmetric, but $\phi(z)$ is symmetric; this is a qualitative difference between results for the cases of twist and no twist.

5. Nematics with negative diamagnetic anisotropy ($\chi_A < 0$)

So far the material has been assumed to have positive diamagnetic anisotropy. In such a case the director field tends to align parallel to the applied magnetic field. When the nematic has negative diamagnetic anisotropy, **H** tries to push the director field into a plane normal to **H**. Naturally, the nature of the variation of distortion with magnetic tilt can be expected to be different from that studied in previous sections. It is indeed known [18] that application of the magnetic field along certain directions can lead to different kinds of instabilities in a negative χ_A material having an undistorted ground state. It should be interesting, therefore, to find out what happens when the ground state of such a material is distorted (either S_1 or S_2).

For ease of comparison with earlier results, the material parameters of E7 (11) are used, except that χ_A is taken negative. When the ground state is a simple twisted nematic, there exists no threshold field of deformation with **H** along the z axis. For the sake of uniformity, however, the reduced field R is defined as in (10) with the sign of χ_A reversed in (9). The boundary tilt is taken as $\theta_0 = 0{\cdot}05$ radian throughout.

In the earlier study, the α range of $0 \leqslant \alpha \leqslant \pi$ had been employed. As the boundary tilt is small, this is almost the same as $\theta_0 \leqslant \alpha \leqslant \pi + \theta_0$. In the present case of a negative χ_A material, it seems reasonable [18] to fix the α range shifted with reference to the earlier one by $\pi/2$; i.e., $\theta_0 - \pi/2 \leqslant \alpha \leqslant \theta_0 + \pi/2$. In the same way, the β range of variation at a given α is fixed as $-\pi/2 \leqslant \beta \leqslant \pi/2$.

We start with the S_1 ground state (7); calculations are presented for one sufficiently elevated value of the ground state twist ($\phi_0 = 1{\cdot}56$ radian; see figure 10). It is seen that when β is sufficiently low (see figures 10 (*a*)–(*d*)), the variation of deformation with the magnetic polar angle α follows either the Type *A* (when the field is weak) or the Type *D*

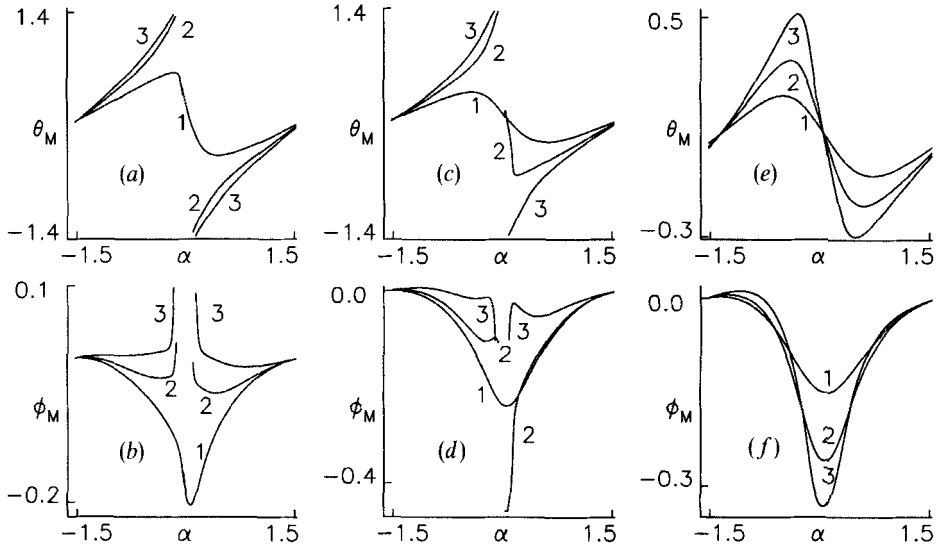

Figure 10. Variation of θ_M and ϕ_M with α for a nematic with $\chi_A < 0$. The elastic constants are those of E7. The reduced field R is defined as in (10) by reversing the sign of χ_A in (9). The ground state is S_1 (8) with $\phi_0 = 1{\cdot}56$ radian (total twist close to π) and director boundary tilt $\theta_0 = 0{\cdot}05$. The magnetic azimuthal angle $\beta = (a)$ and (b) 0·39 (c) and (d) 0·78 (e) and (f) 1·17. $R = (1)$ 1·0 (2) 1·5 (3) 2·0. When a strong field is applied at low β (a)–(d) the Type *D* variation results, indicating the possibility that the deformation may change over to the S_2 type near the gap edges (see § 5).

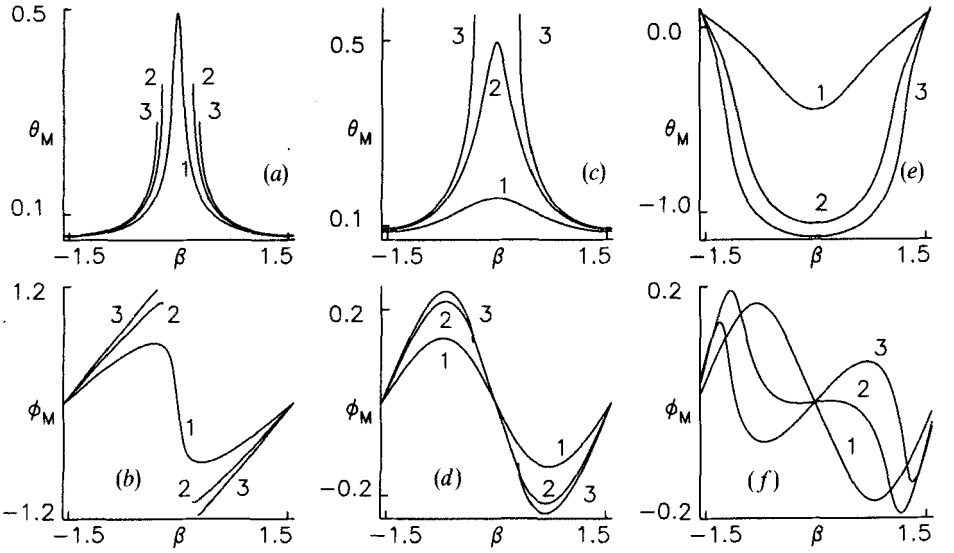

Figure 11. Plots of θ_M and ϕ_M versus β for a negative χ_A nematic. S_1 ground state. Material parameters and R defined as in figure 10. $R=(1)$ 1·0 (2) 1·5 (3) 2·0 in (*a*) and (*b*). $R=(1)$ 0·75 (2) 0·95 (3) 1·0 in (*c*) and (*d*). $R=(1)$ 1·0 (2) 2·0 (3) 3·0 in (*e*) and (*f*). The figures are drawn for $\phi_0=(a,b)$ 0·78 (*c*)–(*f*) 1·56 radian. The magnetic polar angle $\alpha_0=(a)$–(*d*) 0·0 (*e*–*f*) 0·39 radian. Type *D* variation exists when a strong **H** is applied in the *xy* plane; when **H** is tilted away from the *xy* plane, only Type *A* variation seems to occur (see § 5).

(for strong fields) pattern. The possibility of observing the Type *B* variation for intermediate field strengths cannot be ruled out, but this range of R has not been carefully investigated. Interestingly, the nature of the variation changes rather sharply when β is high enough (see figures 10 (*e*) and (*f*)); for the same range of field strengths, only Type *A* variation is seen with θ_M and ϕ_M becoming single valued functions of α. When the variation is of Type *D* (with the S_1 deformation not existing over a gap width near the centre of the α range), the possibility of an irreversible change to S_2 distortion with much lower total twist may be expected.

Figure 11, which shows the variation of the magnetic azimuthal angle, conveys a similar message. When a strong field **H** lies in the *xy* plane ($\alpha=0$), the Type D variation is encountered, showing a change over to S_2. When α is increased by a small amount, the variation switches over to Type *A* even at elevated field strengths. Considering the oscillations which occur in ϕ_M, it seems interesting to make optical observations in this case.

Figures 12 and 13 contain results on the S_2 solution. It is seen that the main results are qualitatively similar to those of the case of a nematic with positive χ_A. For instance, when the total twist is high enough and the field sufficiently strong one observes the Type *D* pattern of variation with the S_2 solution becoming non-existent over a gap width near the centre of the α or β range; clearly, a transition to S_1 is expected at the edges of the gap. The other features to be noted are in the β variation. It is found (see figures 13 (*a*) and (*b*)) that a threshold-like behaviour seen in the positive χ_A material (see figures 7 (*a*) and (*b*)) is to be found in the present case too, when β assumes the extremities of its range ($\beta=\pm\pi/2$); at these β values it may be seen that the deformation becomes non-symmetrical when the field strength is increased beyond a critical value. Needless to say, calculations of threshold at these two β values should lead to

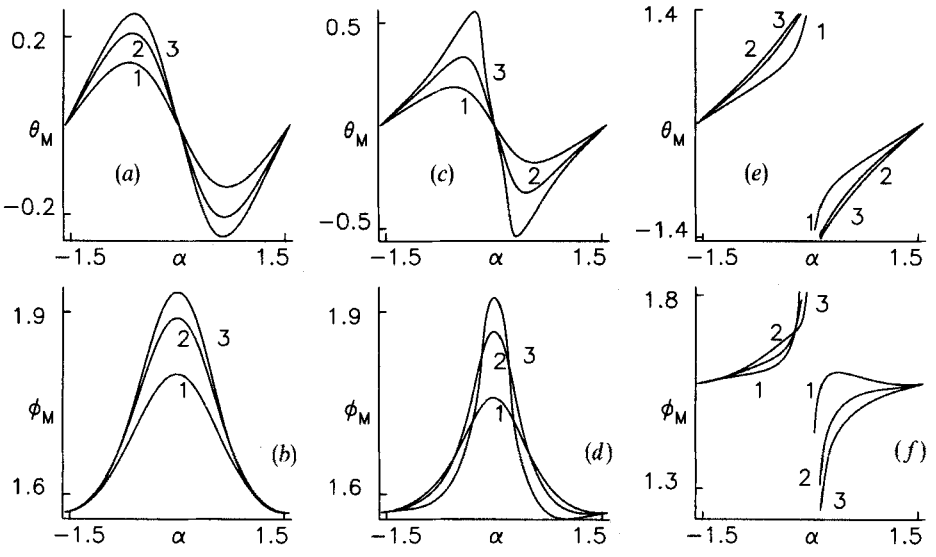

Figure 12. Variations of θ_M and ϕ_M with the magnetic polar angle α for a negative χ_A material with parameters as in figure 10. The solution studied is of S_2 type with director tilt at the sample planes $\theta_0 = 0{\cdot}05$ radian and overall twist $= \pi - 2\phi_0$. $\phi_0 = (a)$ and (b) 0·39 (c)–(f) 0·0 radian. The reduced field R is defined as in figure 10. Curves are drawn for $R = (1)$ 1·0 (2) 1·5 (3) 2·0. The magnetic azimuthal angle $\beta = (a)$–(d) 0·39 (c) and (f) 1·17. It is found that when β is high enough and the overall twist sufficiently pronounced (e) and (f) solutions satisfying (20) do not appear to exist over a gap near the centre of the α range, strongly suggesting a transition at the edges of the gap to the S_1 solution carrying significantly lower total twist (see § 5).

conclusions that are qualitatively similar to those depicted in figure 9; however, detailed calculations cannot be presented here. The other aspect which is worth noting is the change in sign of the curvature of the θ_M curves when α is increased from zero (compare the shapes of the curves in figure 13 (a) with those in figures 13 (c) and (e).

6. Conclusions

The effect of changing the magnetic tilt at constant field strength on the deformation in a (non-chiral) nematic sample is the main subject of the present work. When the director is tilted at the boundaries and an overall twist is imposed, two (topologically inequivalent) ground states are possible and these have been named S_1 and S_2. When the total twist is not high, the distortion variation with magnetic tilt follows one of the three patterns discussed in earlier work. When the twist is considerable, however, a fourth type of variation (Type D) is encountered such that on starting with one of the ground states, say the S_1, solutions satisfying the boundary conditions for S_1 cannot be found over a gap near the centre of the range of magnetic tilt; it is suggested that an irreversible transition to the S_2 solution may occur when the magnetic tilt crosses either edge of the gap. A similar conclusion may be drawn if one starts with the S_2 ground state endowed with considerable twist. This is immediately seen as a natural consequence of the material being non-chiral (having no intrinsic twist); whatever twist exists is imposed through rotations of the sample planes about the sample normal. When the total twist is large, the director deformation becomes potentially unstable against perturbations when the magnetic field strength and tilt

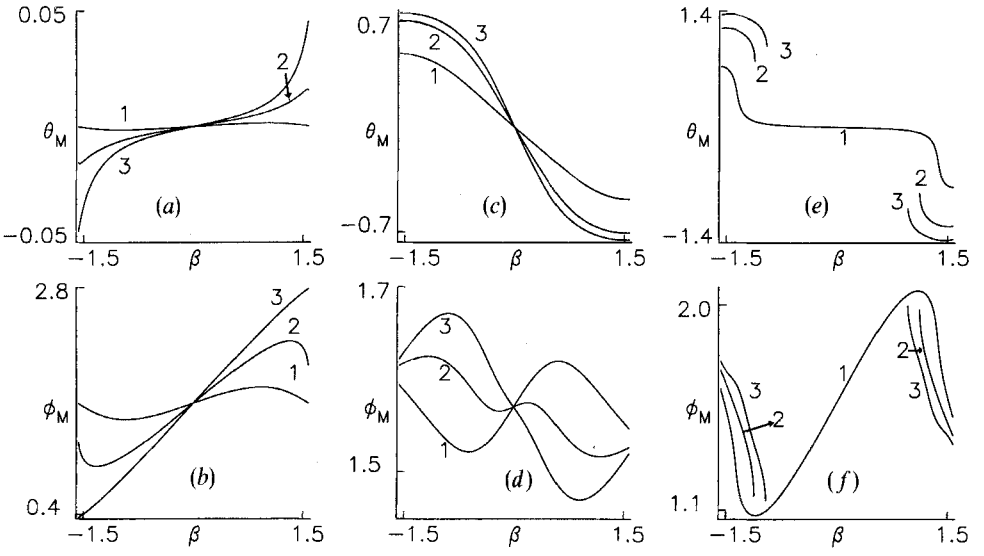

Figure 13. θ_M and ϕ_M versus β, the magnetic azimuthal angle for the S_2 deformation in a negative χ_A nematic. For definitions of the reduced field R and values of material parameters, see figure 10. The total twist is $\pi - 2\phi_0$ with $\phi_0 = (a)$ and (b) 1·17 (c) and (d) 0·0 (e) and (f) 0·39. The magnetic polar angle $\alpha = (a) = (b)$ 0·0 (c) and (d) 0·78 (e) and (f) 0·05. The curves are drawn for $R = (1)$ 0·5 (2) 1·0 (3) 1·5 in (a) and (b). $R = (1)$ 1·0 (2) 2·0 (3) 3·0 in (c) and (d). $R = (1)$ 1·0 (2) 1·25 (3) 1·5 in (e) and (f). It may be observed (a) and (b) that at the extremities of the β range the deformation retains the symmetries of the S_2 solution only for weak fields; when the field strength is enhanced, a non-symmetrical solution results (compare with figures 7 (a) and (b) and figure 9). When the total twist is high enough, the distortion may make an irreversible transition from the S_2 to the S_1 type near the gap edges (see § 5).

assume suitable values. Thus, time dependent linear perturbations tend to grow near the edges of the gap and this lends credence to the hypothesis. The above results for a positive χ_A nematic are found to be substantially true even for a negative χ_A material; in particular, the Type D variation of deformation is again seen under similar conditions.

Calculation for the S_1 solution have been presented in some detail by studying nematics with different elastic ratios. While the elastic ratio does affect the stability of the ground state, it is found that magnetic field effects are quite similar for different materials. In the case of the S_2 solution, one encounters a transition when the strength of the applied field is increased with the field impressed along specific directions. Up to a threshold value of the field strength, the deformation changes, retaining the symmetries of the ground state; when the field strength exceeds the threshold value, the distortion becomes non-symmetric. This threshold has been estimated by employing a time independant perturbation analysis for different sets of parameters. Such a transition has been known for some time [28]; the present work seeks to show that the transition may occur even for general field orientations.

It may be advisable to summarize the assumptions made in this work which, in some cases, do constitute a limitation. Firstly, the rigid anchoring hypothesis is used. This essentially means that regardless of the field strength, the director orientation at

the sample planes remains the same as that dictated by the easy direction. This assumption has a simplifying effect in that the actual values of the sample thickness and χ_A become immaterial and results can be expressed by defining a suitable reduced field. In particular, it may be said that for given boundary conditions of the director, the results are valid for any sample thickness at the same value of the reduced field. But it must be remembered that in a real situation the director anchoring is never rigid [21]. When a field is applied to a nematic sample, under the action of the elastic torque exerted at the sample planes, the director orientation at the boundaries can change. It is natural, therefore, that sample thickness as well as the director anchoring strengths should become parameters to be reckoned in more realistic calculations; this should be of especial importance when the sample thickness is comparable to the extrapolation length. However, the present calculations can be assumed to be valid for sufficiently thick samples even in cases where the director anchoring energy at the sample boundaries is finite.

A situation where the presence of weak anchoring can be felt will be the one (involving Type *D* variation) where the solution changes from S_1 to S_2 or vice versa. Once the change over has occurred at a given magnetic tilt, it is quite likely that the director tilt at the boundaries will also be affected. This should be expected as the change in the nature of the deformation is accompanied by a severe reduction in the overall twist in the sample. Needless to say, anchoring energy will also influence the magnitudes of the growth rates of the perturbations.

One of the effects of weak anchoring will be in defining the domains of definitions of the S_1 and S_2 ground states. A convenient way of preparing these ground states is to start with the director confined to a single plane normal to the sample boundaries and subsequently imparting the necessary amount of twist by rotating the sample planes about the sample normal. During this process, bulk elastic torques come into the picture and these will exert a torque on the director field at the sample boundaries; if the anchoring is weak, the director alignment at the sample planes can change and this can be expected to affect the domain of stability of the ground state.

The linear perturbation analysis essentially reduces to an eigenvalue problem in which the absolute magnitudes of the perturbations are not known. It is not possible to predict the exact direction in which the distortion changes after an instability sets in. This becomes possible only if we solve the exact non-linear equations which link temporal and spatial derivatives of the director field with the velocity gradients (see, for instance equations 4.3 and 4.4 in [18]). It seems possible to conclude, as before [17, 18], that the time of transition at the edges of the bistable regions (for Type *B* variation) should increase as the square of the sample thickness when the anchoring is rigid. It should be interesting to find out how the time or transition behaves when the distortion variation is of Type *D*; at the gap edges when the nature of the solution changes from S_1 to S_2 or vice versa, will the time of transition still vary as the square of the sample thickness?

While mentioning domain formation, it may be necessary to raise a question related to the existence of the ground states even in the limit of the rigid anchoring hypothesis (see discussion at the end of §4.3.). It has been assumed that the ground state has a mono-domain, homogeneous distortion. While this may be a reasonable assumption in the case of the S_1 ground state, one is not sure about S_2; it appears that experiment will have to show the way.

When the original static configuration becomes unstable and the perturbations grow, the uncertainty about the absolute magnitudes of the perturbations leads to the

possibility of domain formation. At the edges of the bistable region (Type *B* variation) where the distortion suffers a transition from one branch to another or at the edges of the gap (Type *D* variation) where the deformation changes from S_1 to S_2 or vice versa, the possibility of domain formation must be borne in mind. In the present work, as the director field has been assumed to be a function of only one spatial coordinate, it has not been possible to study different domains simultaneously. This fact must be born in mind while considering the results of figures 8 and 9 on the threshold r_C.

It has been recently shown [29] that when the anchoring is weak and the applied field strong enough, the director field in a nematic sample can get oriented parallel to **H**. The expression for the threshold aligning field has also been calculated for special directions of **H** relative to the sample normal. Earlier studies on bistability in weakly anchored nematics [17] have indicated similar possibilities. In the light of these results, a study of the effects of anchoring strength in the present case assume especial significance. It should also be remembered that when the director orientation is specified by two angles as in the present case, it may be necessary to consider both the polar and the azimuthal anchoring strengths when the anchoring energy is finite.

Another aspect that presents itself for study is the optical property of the sample (for instance, the phase retardation or the transmitted intensity between crossed polarizers, etc.). It has been demonstrated [29] for a simple geometry that even when the variation of distortion with magnetic tilt looks symmetric with respect to the centre of the range of magnetic tilt, the optical properties of the nematic cell may vary most asymmetrically. Considering the different shapes assumed by the deformation curves in the present work, it seems appropriate to expect that a study of optical properties in the present case will prove fruitful.

All the above studies have been made in the static limit. It has been assumed that each time the magnetic field or tilt is varied in small steps, sufficient time is given to the system to attain a new state of equilibrium. It has been pointed out [17, 18] that extending the above studies to a magnetic field (or the sample) rotating at some constant rate should prove instructive, as this might lead to the observation of novel flow patterns as has, indeed, been done earlier in many simpler geometries (see, for instance, [30]). Independently, such experiments have been reported recently [31] on polymer nematic materials and new flow patterns observed; these investigators have employed the simplest possible ground state for their experiments and have also spun the magnetic field about an axis parallel to the sample planes, but normal to the initial direction of alignment. It should be interesting to extend this study to low molecular weight compounds with particular emphasis on the effect of changing the tilt of the magnetic plane. When the boundary director is tilted, it may be possible to compare results for S_1 and S_2 ground states in both the high twist and the low twist regimes.

Though the governing equations were derived to represent a chiral nematic (or cholesteric), the intrinsic chirality has been equated to zero in this work. When the material is chiral, the equilibrium pitch of periodicity enters the picture and its ratio with the sample thickness appears as an additional parameter. Because of this, results have to be presented for different sample thicknesses even in the rigid anchoring limit. Preliminary calculations show that the presence of chirality is likely to affect the qualitative nature of the results. It is found that at comparable values of the reduced field, for example, one gets Type *A* variation for a chiral material, while one had Type *B* variation for the non-chiral case; Type *D* variation seems to be absent. Thus, the presence of chirality seems to lend additional stability to the orientation pattern. In a sense, this is to be expected from the empirical fact that supertwisted nematic displays

work; it is the extra 'spring' due to the presence of intrinsic chirality that enables the ground state to be attained in the off state.

Another fact has to be borne in mind while studying systems with intrinsic chirality. When such a sample of sufficiently short pitch is aligned with the helical axis normal to the plates, the deformation produced by applying a magnetic field parallel to the sample boundaries will be homogeneous, while that induced by impressing the field normal to the plates is periodic. This means that if we start with the field in the sample plane and tilt the field towards the sample normal, there should be a critical tilt beyond which the homogeneous distortion should disappear; a preliminary study shows that this actually happens. Detailed calculations for this case will be presented in the future.

References

[1] OSEEN, C. W., 1933, *Trans, Faraday Soc.*, **29,** 883. FRANK, F. C., 1958, *Discuss. Faraday Soc.*, **25,** 19.

[2] ERICKSEN, J. L., 1976, *Advances in Liquid Crystals*, edited by G. H. Brown (Academic Press), p. 233. LESLIE, F. M., 1979, *Advances in Liquid Crystals*, edited by G. H. Brown (Academic Press), p. 1.

[3] DE GENNES, P. G., 1975, *The Physics of Liquid Crystals* (Clarendon Press), Chaps. 3 and 5.

[4] CHANDRASEKHAR, S., 1977, *Liquid Crystals* (Cambridge University Press), Chap. 3.

[5] BLINOV, L. M., 1983, *Electro-optical and Magneto-optical Properties of Liquid Crystals* (John Wiley), Chaps. 3 and 4.

[6] SCHADT, M., and HELFRICH, W., 1971, *Appl. Phys. Lett.*, **18,** 127.

[7] BAHADUR, BIRENDRA (editor), 1990, *Liquid Crystals: Applications and Uses, Vols. 1–3 (World Scientific).*

[8] BERREMAN, D. W., and HEFFNER, W. R., 1981, *J. appl. Phys.*, **52,** 3032.

[9] WATERS, C. M., BRIMMELL, V., and RAYNES, E. P., 1983, *Proceedings of the Third International Display Research Conference*, Kobe, Japan, p. 396. SCHEFFER, T. J., and NEHRING, J., 1984, *Appl. Phys. Lett.*, **45,** 1021.

[10] See article by T. Scheffer and J. Nehring in [7].

[11] PORTE, G., and JADOT, J. P., 1978, *J. Phys., Paris*, **39,** 213.

[12] BOYD, G. D., CHENG, J., and NGO, P. D. T., 1980, *Appl. Phys. Lett.*, **36,** 556; for a review on this subject and additional references see, for instance: THURSTON, R. N., 1985, *Molec. Crystals liq. Crystals*, **122,** 1.

[13] FRISKEN, B. J., and PALFFY-MUHORAY, P., 1989, *Phys. Rev.* A, **39,** 1513; 1989, *Ibid.*, **40,** 6099. KINI, U. D., 1990, *Liq. Crystals*, **8,** 745; *J. Phys., Paris*, **51,** 529.

[14] ONNAGAWA, H., and MIYASHITA, K., 1974, *Jap. J. appl. Phys.*, **13,** 1341. MOTOOKA, T., and FUKUHARA, A., 1979, *J. appl. Phys.*, **50,** 3322. KARN, A. J., SHEN, Y. R., and SANTAMATO, E., 1990, *Phys. Rev.* A, **41,** 4510.

[15] OLDANO, C., MIRALDI, E., STRIGAZZI, A., VALEBREGA, P. T., and TROSSI, L., 1984, *J. Phys., Paris*, **45,** 355.

[16] DERFEL, G., 1988, *Liq. Crystals*, **3,** 1411.

[17] KINI, U. D., 1991, *Liq. Crystals*, **10,** 597.

[18] KINI, U. D., 1992, *Liq. Crystals*, **12,** 449.

[19] MEYER, R. B., 1968, *Appl. Phys. Lett.*, **12,** 281; LESLIE, F. M., 1970, *Molec. Crystals liq. Crystals*, **12,** 57.

[20] HELFRICH, W., 1971, *J. chem. Phys.*, **55,** 839; RONDELEZ, F., and HULIN, J. P., 1972, *Solid St. Commun.*, **10,** 1009.

[21] RAPINI, A., and PAPOULAR, M., 1969, *J. Phys. Colloq., Paris*, **30,** C4–54. GUYON, E., and URBACH, W., 1976, *Nonemissive Electro-optic Displays*, edited by A. R. Kmetz and F. K. von Willisen (Plenum Press), p. 121; COGNARD, J.,1982, *Molec. Crystals liq. Crystals Suppl.*, **1,** 1.

[22] FINLAYSON, B. A., 1972, *The Method of Weighted Residuals and Variational Principles* (Academic Press), Chap. 5. TSENG, H. C., SILVER, D. L., and FINLAYSON, B. A., 1972, *Physics Fluids*, **15,** 1213.

[23] ABRAMOWITZ, M., and STEGUN, I. A., (editors) 1972, *Handbook of Mathematical Functions* (Dover), Chap. 25.

[24] BERREMAN, D. W., 1980, *The Physics and Chemistry of Liquid Crystals Devices*, edited by G. J. Sprokel (Plenum Press), p. 1.
[25] CHEN, G. P., TAKEZOE, H., and FUKUDA, A., 1989, *Liq. Crystals*, **5**, 341.
[26] FRASER, C., 1978, *J. Phys.* A, **11**, 1439.
[27] KINI, U. D., 1993, *J. Phys., Paris II*, **1**, 225.
[28] CHENG, J., THURSTON, R. N., and BERREMAN, D. W., 1981, *J. appl. Phys.*, **52**, 2756.
[29] KINI, U. D., 1993, *Liq. Crystals*, **13**, 735.
[30] MIGLER, K. B., and MEYER, R. B., 1991, *Phys. Rev. Lett.*, **66**, 1485; see [18] for other references.
[31] SCHWENK, N., BOEFFEL, C., and SPIESS, H. W., 1992, *Liq. Crystals*, **12**, 735.